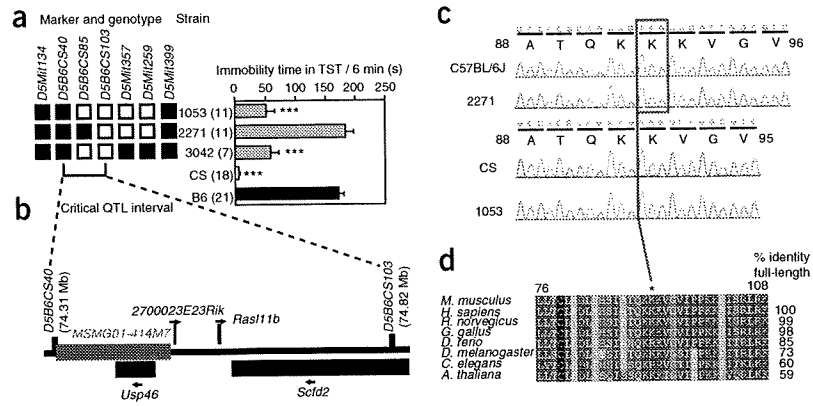

Figure 2 Identifying the quantitative trait gene on mouse chromosome 5 that influences TST immobility time. (**a**) Genotype and the immobility time on TST in the B6.CS-Ngu1053 (1053), B6.CS-Ngu2271 (2271) and B6.CS-Ngu3042 (3042) strains that define the critical QTL interval. The solid and open boxes represent the B6 and CS alleles, respectively, and 1053, 3042 and CS showed a significantly shorter immobility time than B6 (one-way ANOVA, $F_{4,63} = 81.8$, $P < 9.4 \times 10^{-10}$; Tukey-Kramer *post hoc* test, $^{***}P < 0.001$). The number of mice used is shown within parentheses. (**b**) The genes in the critical QTL interval and the BAC clone (*MSMG01-414M7*) used for transgenic rescue. The arrows indicate the directions of transcription. (**c**) The 3-bp deletion coding for lysine in the open reading frame of *Usp46* in CS and 1053. (**d**) The alignment of the amino acid sequences of the *Usp46* homologs. The region around the deletion of the lysine residue is highly conserved in different species. The sequence identity for the full-length protein is shown. Mouse, NP_808229; human, NP_073743; rat, XP_214034; chicken, XP_420711; zebrafish, NP_001077025; fruitfly, NP_732801; *C. elegans*, P34547; *Arabidopsis*, NP_565532.

© 2009 Nature America, Inc. All rights reserved.

Candidate gene screening

The above-mentioned critical interval contained four or three genes and one expressed sequence tag (EST) gene (*Usp46*, *Rasl11b* and *2700023E23Rik* have been registered as genes in the National Center for Biotechnology Information (NCBI) database; *Scfd2* is located outside the interval as per the NCBI database; *Scfd2* is included in the interval and *1700112M01Rik* is designated as an EST gene in the Ensembl database) (**Fig. 2b**). To identify the responsible gene, we examined the sequence of the coding region of these genes and their expression in the brain by *in situ* hybridization and compared the sequences and gene expression among the B6, CS and B6.CS-Ngu1053 strains (**Supplementary Fig. 3** online). The result revealed only one 3-bp deletion (a lysine codon) in *Usp46* (**Fig. 2c,d**). We found no other differences in the expression sites or levels of this gene. The other genes apparently did not differ in their sequences, expression sites or levels among the three strains (**Supplementary Fig. 3**).

Analysis of transgenic strains

We produced transgenic and nontransgenic progeny with homozygous and heterozygous genotypes (**Fig. 3a**). Southern blot analysis revealed that the bacterial artificial chromosome (BAC) was integrated into the genomes of the founder mice (**Supplementary Fig. 4** online). To confirm *Usp46* transgene expression, we first sequenced the coding region of *Usp46* and detected the single nucleotide polymorphism (SNP) that differed between the MSM/Ms strain and the other two strains (B6 and CS). Using this SNP, we examined mRNA expression in the brains of the transgenic mice with B6 and CS heterozygous alleles (B/C) in the congenic region of the B6.CS-Ngu1053 strain and detected two signals derived from the endogenous allele (B6 and CS) and the transgene (MSM/Ms) (**Fig. 3b**; **Supplementary Fig. 5a** online), which indicated that *Usp46* was expressed in the brains of the transgenic mice. In addition, we investigated *Usp46* expression in the brain by *in situ* hybridization (**Fig. 3c**; **Supplementary Fig. 5b**). *Usp46* was strongly expressed in a number of regions, including the olfactory bulb, cingulum bundle, amygdala, hippocampus and cerebellum in the transgenic strains, although these strains showed different expression levels. As compared with the nontransgenic mice, there were no obvious regional differences in *Usp46* expression.

The *Usp46* transgene (tg) completely rescued the phenotype in both heterozygous (B/C) and CS homozygous (C/C) genotypes; however,

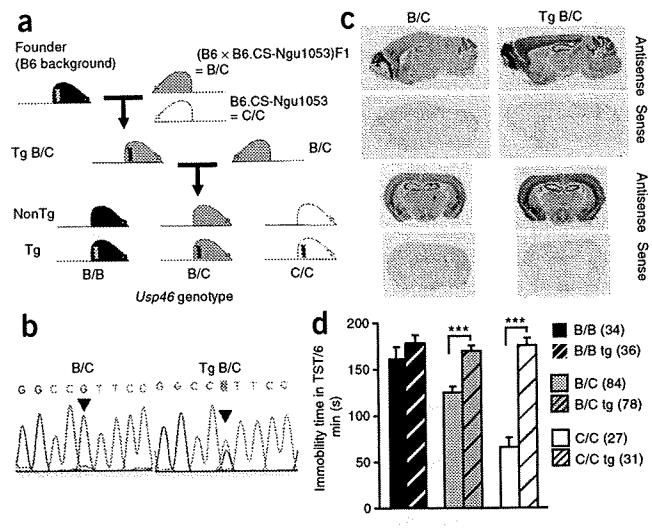

Figure 3 Generations and analysis of BAC transgenic mice. (**a**) The genetic cross used to produce the transgenic F_2 mice. The black, gray and white mice represent the B6 homozygous (B/B), B6 and CS heterozygous (B/C) and the CS homozygous allele (C/C) at the congenic region of the B6.CS-Ngu1053 strain, respectively. The presence of the transgene is indicated by a double helix symbol. Each congenic genotype (B/B, B/C and C/C) was combined with (tg) or without (non tg) the transgene. (**b**) The *Usp46* variant sites are indicated by an arrowhead (B6 and CS, guanine; MSM/Ms, adenine). The SNP is silent and located in exon 3 (174 from the start codon). Two signals derived from the inherent genome (B6 and CS) and the transgene (MSM/Ms) were detected in the transgenic mice. (**c**) *In situ* hybridization analysis of *Usp46* in the coronal and sagittal sections of the transgenic and nontransgenic mice. (**d**) Transgenic rescue of the shortened immobility time on TST. The behavior on TST was assessed in 339 F_2 mice; however, 49 mice, which climbed on their tails[4], were excluded from the data, and therefore 290 F_2 mice were analyzed. The number of mice used is shown within parentheses. Two-way ANOVA was used to detect the effects of the transgene and congenic genotype. Transgene presence: $F_{1,290} = 55.8$, $P < 9.5 \times 10^{-13}$; congenic genotype: $F_{2,290} = 11.7$, $P < 1.3 \times 10^{-5}$. To confirm whether the transgene increases the TST immobility time in the same congenic genotype, Student's *t*-test was performed ($^{***}P < 0.001$). One-way ANOVA was performed to compare the degree of rescue among the different congenic genotypes; however, no differences were found in any pair of congenic genotypes ($F_{2,144} = 0.63$, $P = 0.53$).

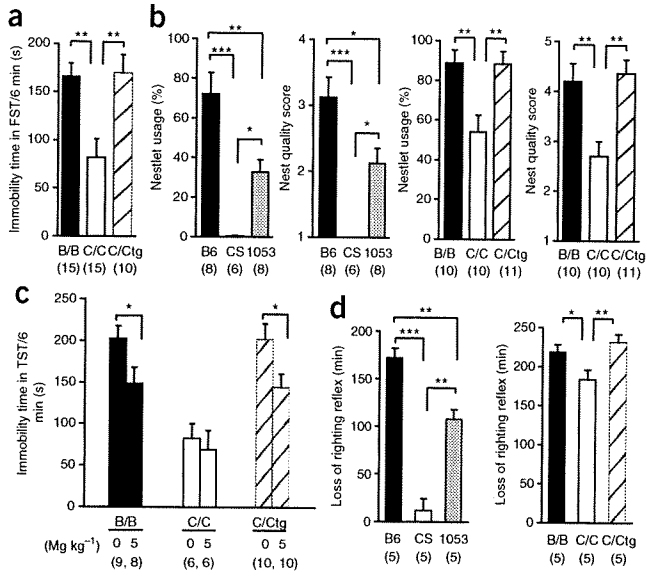

Figure 4 Behavioral pleiotropism of *Usp46* and transgenic rescue. (**a**) Transgenic rescue of the immobility time on FST. The C/C tg strain showed a significantly longer FST immobility time than the C/C strain (one-way ANOVA, $F_{2,37} = 7.1$, $P < 0.0025$). (**b**) The CS and B6.CS-Ngu1053 mice showed a significantly lower nest usage ($F_{2,19} = 19.8$, $P < 2.3 \times 10^{-5}$) and nest quality score ($F_{2,19} = 19.0$, $P < 3.0 \times 10^{-5}$) than the B6 mice. The C/C tg strain showed a significantly higher level of nest usage ($F_{2,28} = 7.2$, $P < 0.0031$) and nest quality score ($F_{2,28} = 8.5$, $P < 0.0013$) than the C/C strain. (**c**) Imipramine administration reduced the immobility time on TST in the B/B and C/C tg strain (B/B, $P < 0.039$; C/C tg, $P < 0.034$), but not in the C/C strain. (**d**) Duration of the loss of righting reflex after administration of muscimol (3 mg kg^{-1}). The CS and B6.CS-Ngu1053 strains showed a significantly shorter duration than the B6 strain (one-way ANOVA, $F_{2,12} = 56.9$, $P < 7.6 \times 10^{-7}$). The transgene increased the duration ($F_{2,14} = 8.5$, $P < 0.0039$). The number of mice used is shown within parentheses. Tukey-Kramer *post hoc* test: $^{***}P < 0.001$, $^{**}P < 0.01$, $^{*}P < 0.05$.

this did not affect the immobility time in the B/B genotype (**Fig. 3d** and **Fig. 4a**; **Supplementary Table 4** online).

Behavioral pleiotropism of *Usp46*

To gain insight into the function of *Usp46*, we subjected the B6.CS-Ngu1053 mice to a number of behavioral tests (open-field, light-dark box, elevated plus-maze, hole-board and nest-building tests). The results of the nest-building and light-dark box tests differed significantly between the B6 and B6.CS-Ngu1053 mice (nestlet usage, $P < 0.01$; nest quality score, $P < 0.05$; time in dark box, $P < 0.02$) (**Fig. 4b**; **Supplementary Fig. 6** online). In the nest-building test, the B6 mice used substantial amounts of nest material and B6.CS-Ngu1053 mice used moderate amounts of nest material, whereas virtually no nest material was used by the CS mice. In the light-dark box test, B6.CS-Ngu1053 mice spent less time in the dark compartment than B6 mice, but the number of times the mice defecated was similar in these strains (defecation, 0.33 ± 0.18 for B6, 0 ± 0 for B6.CS-Ngu1053; $P = 0.11$, Mann-Whitney U test). In addition, we examined the effects of the administration of the antidepressant drug imipramine on the TST immobility time to assess the role of *Usp46* in the antidepressant activity of imipramine. Although imipramine administration significantly reduced immobility time in the B/B strain, no obvious effects were observed in the C/C strain (**Fig. 4c**). The *Usp46* transgene completely rescued the nest-building behavior and the insensitivity to the anti-immobility effects of imipramine (**Fig. 4**).

Involvement of *Usp46* in the regulation of the action of GABA

Because CS mice did not exhibit immobility in the TST and FST, we assumed that the inhibitory action on the behavior might be attenuated. To test this assumption, we first measured the sensitivity to muscimol, a selective $GABA_A$ receptor agonist and a partial agonist for $GABA_C$ receptors, in *Usp46* mutant mice. Because muscimol administration eliminated the righting reflex, we analyzed the duration of loss of the righting reflex. The results revealed that the recovery of the righting reflex was extremely fast in the CS mice ($P < 0.001$ versus B6), and this characteristic was also observed in the B6.CS-Ngu1053 mice ($P < 0.01$ versus B6). The idea that *Usp46* is involved in the attenuated sensitivity to muscimol is supported by the results of the rescue experiment (**Fig. 4d**).

To directly determine whether the *Usp46* mutation indeed altered the $GABA_A$ receptor–mediated inhibitory current, we obtained whole-cell patch-clamp recordings from CA1 pyramidal neurons of the hippocampus, one of the brain regions that strongly expressed *Usp46* as shown by *in situ* hybridization, in slice preparations from the mice with the three genotypes. First, we found no statistical differences in the resting membrane potentials (B/B, –72.7 ± 1.4 mV; C/C, –72.4 ± 1.1 mV; C/C tg, –71.9 ± 1.4 mV) and input resistances (B/B, 134 ± 9.3 MΩ; C/C, 148 ± 9.3 MΩ; C/C tg, 132 ± 8.8 MΩ) of the cells among the three mouse strains. Next, the $GABA_A$ receptor–mediated muscimol currents were recorded by the consecutive application of 0.1, 1.0 and 10.0 μM muscimol. Notably, the muscimol-induced outward current in the cells from the C/C strain was the lowest among all the mice strains at all concentrations examined (**Fig. 5a**). Lastly, we performed miniature inhibitory postsynaptic current (mIPSC) analysis on the same CA1 pyramidal neurons. However, we found no significant differences in the amplitude, rise time, decay time or frequency of the mIPSCs among the three strains of mice (**Fig. 5b**).

Immunohistochemistry

To further study the involvement of *Usp46* in the GABAergic system, we examined the expression of the 67-kDa isoform of glutamic acid

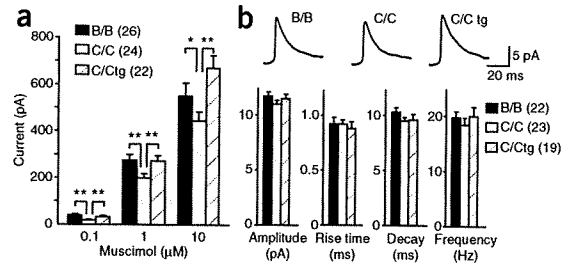

Figure 5 *Usp46* mutation reduces muscimol-induced $GABA_A$ receptor–mediated currents but preserves GABAergic mIPSCs. (**a**) Muscimol-induced currents recorded from CA1 pyramidal neurons. The C/C strain showed a significantly lower amount of muscimol-induced currents than the B/B and C/C tg strains (one-way ANOVA, 0.1 μM: $F_{2,69} = 7.60$, $P < 0.001$; 1 μM: $F_{2,69} = 4.00$, $P < 0.023$; 10 μM: $F_{2,69} = 5.25$, $P = 0.0076$). (**b**) GABAergic mIPSCs in the B/B, C/C and C/C tg strains were not significantly different from each other in amplitude, 20–80% rise time, decay time and frequency. Upper traces are representative mIPSCs of CA1 pyramidal neurons in the three genotypes. Each trace was obtained by averaging the mIPSCs that occurred in a 3-min time window. The number of cells recorded is shown within parentheses (19–26 cells from 4–5 mice; age, 33–41-days-old). Student's *t*-test with Bonferroni correction: $^{**}P < 0.01$, $^{*}P < 0.05$.

© 2009 Nature America, Inc. All rights reserved.

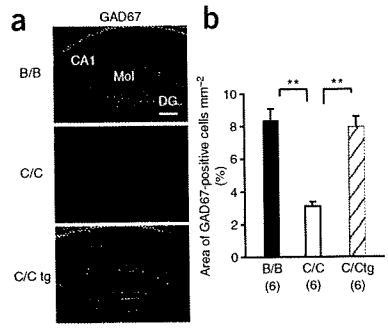

Figure 6 *Usp46* mutation reduces GAD67 immunostaining in the hippocampus. (**a**) Immnostaining against GAD67 in the hippocampus of the B/B, C/C and C/C tg strains. CA1, Cornet d'Ammon 1; DG, dentate gyrus; Mol, molecular layer in the DG; scale bar, 200 μm. (**b**) Quantification of GAD67 expression in the hippocampus of the B/B, C/C and C/C tg strains. The area of GAD67-positive cells mm^{-2} in the hippocampus was significantly decreased in the C/C strain compared with the B/B and C/C tg strains (one-way ANOVA, $F_{2,17} = 23.8$, $P < 2.3 \times 10^{-5}$). $^{**}P < 0.01$.

decarboxylase (GAD67, one of the GABA synthetic enzymes) in the hippocampus by immunohistochemistry[23]. Immunoreactivities against GAD67 were significantly lower (especially in the CA1 region and dentate gyrus in the hippocampus) in the C/C strain relative to the B/B strain, and the immunoreactive phenotype was completely rescued in the C/C tg strain (**Fig. 6**).

DISCUSSION

In the present study, we found that the CS mice showed negligible immobility in the TST and FST. Although in some studies, gender differences in the TST and FST were reported[4,24], both male and female CS mice showed virtually no immobile posture. These characteristics of the TST and FST have not been reported in any inbred mice, even in the genetically modified mice[3]. This unusual characteristic is probably due to a multiple gene system consisting of major (chromosomes 5 and 4) and minor QTLs that act in concert to accelerate the mobility. In fact, a congenic strain with a QTL on chromosome 5 showed intermediate levels in these behavioral tests.

Several groups have already sought to map the QTLs that affect the basal immobility time and the antidepressant response in the TST and FST[7–11]. Notably, two recently reported QTLs that influence the immobility time in the TST overlap with our suggested QTLs on chromosome 4. In particular, one peak position reported previously is very similar to that found in our study[8,10].

Using congenic strains, we narrowed the chromosomal region harboring the quantitative trait gene down to a size of 0.5 Mb. Within this region, 1 EST gene (*1700112M01Rik*) was registered in the Ensembl database. We examined the expression of the EST gene in the brain, but we could not detect any signal by *in situ* hybridization analysis. Sequencing and expression analysis of the other genes located in this critical region led us to the idea that *Usp46* with the 3-bp deletion is the most likely candidate gene. To confirm this, we performed a rescue experiment with transgenic BAC and confirmed that *Usp46* is the quantitative trait gene that affects immobility in the TST and FST. *Usp46*, which encodes a deubiquitinating enzyme, is implicated in the ubiquitin-proteasome system, which is critical for the regulation of many cellular processes. In this system, the pathway involving protein ubiquitination and proteasomal degradation has been the focus of many studies. However, the removal of ubiquitin, which is mediated by deubiquitinating enzymes, has not been well studied[25,26]; thus, little is known regarding the physiological functions of USP46. The present study demonstrates for the first time (to our knowledge) that USP46 functions to regulate several behavioral processes, including basal immobility, the anti-immobility effects of imipramine, nest building and the muscimol-induced righting reflex.

To gain insight into the functions of this enzyme, it should be noted that the muscimol-induced righting reflex is affected by the mutation in *Usp46* and is rescued by the transgene. This result suggests that *Usp46* is involved in the regulation of GABA action. The involvement of *Usp46* in GABAergic mechanisms is supported by results showing that the immobility time in the TST and FST is reduced in mice that lack GABA transporter subtype 1 (GAT1)[27], and by results showing that nesting behavior is impaired in mice deficient in the gene encoding $GABA_A$ receptor subunit β3 (*Gabrb3*)[28] and in mice deficient in the gene encoding $GABA_A$ receptor subunit δ (*Gabrd*)[29]. It is reported that imipramine has similar effects for reducing the immobility time in both the GAT1-knockout mice and the wild-type mice[27]; this result is different from our result that normal *Usp46* is required for anti-immobility effects. Our results suggest that *Usp46* may affect GABAergic systems by mechanisms other than those involving GAT1. It is notable that while mapping QTLs, other investigators[8] also focused on the genes coding for the $GABA_A$ receptor subunits as candidates affecting the immobility time in the TST and FST.

To further understand the involvement of *Usp46* in the GABAergic system, we performed electrophysiological analysis of the hippocampal CA1 pyramidal neurons. No significant changes were observed among the three genotypes (B/B, C/C and C/C tg) in the basic cellular electrophysiological properties such as resting membrane potentials and input resistances; however, we found that the muscimol-induced outward current mediated by $GABA_A$ receptors is significantly (35% at the maximum) decreased in the C/C strain compared with the B/B and C/C tg strains. This finding suggested that the *Usp46* transgene might have rescued the GABAergic responses, thereby normalizing behavioral abnormalities as observed in the C/C tg strain. However, it is unlikely that the $GABA_A$ receptor *per se* is qualitatively altered in the C/C strain, because no differences were found among the three strains with regard to the physiological properties of the $GABA_A$ receptor channel current (such as the amplitude, rise time and decay time). The frequency of mIPSCs depends on the number of synapses and the probability of neurotransmitter release from presynaptic membranes[30], but there were no significant differences in the frequency of mIPSCs among the three strains. Alternatively, it could be argued that changes in the number of extrasynaptic $GABA_A$ receptors cause diminished muscimol-induced current responses in the C/C strain[31].

The involvement of *Usp46* in the GABAergic system is further supported by a marked reduction in GAD67 expression, as determined by immunohistochemistry. Because GAD67 catalyzes the decarboxylation of glutamate to GABA, *Usp46* seems to be involved in GABA synthesis. However, unlike in the GABA-producing neurons, the electrophysiological changes were observed in the hippocampal CA1 pyramidal neurons, which are excitatory neurons. Thus, it is likely that *Usp46* mutation extensively affects the GABAergic system. The pre- and postsynaptic changes observed in these experiments might be explained by the developmental defects caused by a reduction in the levels of GABA, which acts as a neurotrophic factor. It is known that GABA affects several developmental processes of the nervous system, such as proliferation, migration, differentiation, synaptic maturation and cell death[23,32,33]. These changes might lead to the diminished responses to muscimol in the *Usp46* mutant mice. Another interpretation might be that *Usp46* regulates different protein substrates, which independently affect the pre- and postsynaptic

© 2009 Nature America, Inc. All rights reserved.

events. In any case, further investigation is clearly needed to determine how the *Usp46* transgene affects the GABAergic system.

In summary, we identified *Usp46* as a quantitative trait gene responsible for the immobility in the TST and FST. Because *Usp46* appears to be implicated in a wide range of behavioral functions regulated by the GABAergic system, the present results might contribute to the understanding of the neural and genetic mechanisms that underlie the mental disorders associated with this gene.

METHODS

Animals. We purchased the C57BL/6J (B6) mice from CLEA Japan Inc., and CS mice were originally provided by T. Namikawa (Nagoya University). The mice were housed under a 12-h light and dark cycle (LD 12:12, 7:00 on, 19:00 off) with free access to food and water in our animal facility at a temperature maintained at approximately 24 °C. We performed TST and FST on both male and female mice aged 8–12 weeks. The other tests were conducted only on male mice aged 9–24 weeks.

For all the experiments, the animals were treated in accordance with the guidelines issued by Nagoya University, Faculty of Pharmaceutical Sciences of Meijo University and Tokyo Metropolitan Institute of Gerontology.

QTL analysis. Initially, we performed interval mapping using a least-squares regression method (Map Manager QTXb20) on 203 F_2 hybrids (105 male, 98 female) produced by intercrossing F_1 mice obtained from B6 and CS mice using 56 Mit markers (2 to 3 markers per chromosome) purchased from Research Genetics Inc. When significant QTLs were detected, we conducted further analysis using additional markers ($n = 69$) for flanking potential QTLs (**Supplementary Table 5** online). The likelihood of odds (LOD) scores at genome-wide significance (5%) and suggestive (63%) levels were determined by 1,000 runs of a permutation test[34]. The LOD scores at the genome-wide significance (5%) and suggestive (63%) levels for TST and FST were 3.30 and 1.95, respectively. To confirm the presence of the main-effect QTLs detected using Map Manager QTXb20, we performed nonparametric interval mapping using the computer package R/qtl version 1.08-56 (ref. 35), because of the extreme skew in the distribution of both traits (**Fig. 1a**). Epistatic interaction analysis was performed using Map Manager QTXb20, as described previously[36]. The significance of the overall effect was examined by 1,000 runs of a permutation test using Map Manager QTXb20.

Congenic strains. Congenic strains were developed by continually backcrossing (at least six times) a donor strain that harbors the genomic region of interest with B6 by a marker-assisted breeding strategy[37]. We used Mit SSLP markers (**Supplementary Table 5**); however, if no known polymorphic markers existed, we identified long di- or trinucleotide repeats in the genomic sequence and designed primers to amplify these regions. These markers were named *D5B6CS* (**Supplementary Table 6** online). We developed 17 congenic or subcongenic strains on a B6 genetic background that contained various chromosome 5 regions of the CS mice from the Mit marker *D5Mit300* (51.8 Mb) to *D5Mit259* (89.70 Mb) (**Supplementary Fig. 2**). We named these strains B6.CS-Ngu and so on based on the Mouse Genome Informatics guidelines for nomenclature of mouse strains.

Candidate gene analysis. The sequence of each gene in the B6 mice was obtained from Mouse Genome Informatics (http://www.informatics.jax.org/), and primers were designed to amplify the full-length open reading frame (ORF). We carried out sequencing analysis to detect mutations in CS and B6.CS-Ngu1053 in comparison with B6. Total RNA was extracted from the whole brain using TRIzol reagents (Invitrogen). Superscript III reverse transcriptase (Invitrogen) and total RNA with oligo(dT) were used for first-strand complementary DNA synthesis, and candidate genes containing the full-length ORF were amplified by PCR and directly sequenced using the Big Dye cycle sequencing kit (Applied Biosystems) on an ABI 3130 automated sequencer. Because *2700023E23Rik* showed a very low expression level in the brain, we amplified the putative ORF from the genomic DNA. The primers obtained by the amplification of the ORF are listed in **Supplementary Table 7** online.

We carried out *in situ* hybridization to compare the mRNA expression levels among the B6, CS and B6.CS-Ngu1053 strains. We killed the animals by decapitation, and we immediately removed the brains to avoid acute changes in gene expression. *In situ* hybridization was carried out as described previously[38]. Antisense 45-nucleotide oligonucleotide probes were labeled with [^{33}P]dATP (NEN) using terminal deoxyribonucleotidyl transferase (Gibco BRL). Hybridization was carried out overnight at 42 °C. After the glass slides were washed, they were air-dried and apposed to a Biomax-MR film (Eastman Kodak Co.) for 2 weeks with ^{14}C standards (American Radiolabeled Chemicals). The relative optical densities were measured using a computed image-analyzing system (Image Gauge) and were converted into the respective relative radioactive values (nCi) by ^{14}C standards. Specific hybridization signals were obtained by subtracting the background values obtained from the adjacent brain areas that did not exhibit hybridization signals. The oligonucleotide probes are listed in **Supplementary Table 7**.

Transgenic strain. To obtain the transgenic mice for the behavioral tests, we first generated the B6 founder mice having the *Usp46* transgene. These mice were crossed with mice homozygous (C/C) or heterozygous (B/C) for the allele at the congenic region of the B6.CS-Ngu1053 strain. The heterozygous mice with the *Usp46* transgene obtained by this cross were then crossed with B6.CS-Ngu1053 heterozygous mice, producing six different genetic constitutions in the progeny (**Fig. 3a**).

The mouse BAC clone (*MSMG01-414M7*, 74.31–74.48 Mb) originating from the MSM/Ms strain covering the *Usp46* locus (including 12,163 bp upstream and 81,996 bp downstream from the 5′ and 3′ ends) was obtained from RIKEN BioResource Center. We cloned genomic DNA into the pBACe3.6 vector at the EcoRI and EcoRI methylase cloning sites[39]. We obtained BAC DNA from 500 ml of LB using 12.5 μg ml^{-1} chloramphenicol and a NucleoBond BAC 100 kit (MACHEREY-NAGEL) according to the supplier's instructions. To separate the 162-kb MSM/Ms-derived DNA from the vector sequence, the circular BAC clone was digested with NotI (Takara), and the restriction fragments were separated using pulsed-field gel electrophoresis (PFGE) for 18 h on 1% pulse field certified agarose (BioRad) gel under the following conditions: included angle, 120°; 6 V cm^{-1}; and switch-time ramping from 0.1 s to 12 s (CHEF Mapper II, BioRad). After the PFGE run, the marker lanes on either side of the preparative lane and up to ~5 mm were cut off and stained with ethidium bromide. The position of the BAC band was marked with a sterile razor blade, and the part of the preparative lane containing the BAC DNA was excised. The excised gel slice was dialyzed in TE buffer.

The isolated BAC DNA was injected at a concentration of 1 ng μl^{-1} into fertilized mouse oocytes isolated from B6 mating. Oocytes that survived injection were transferred later on the same day to both oviducts of pseudo-pregnant ICR foster mothers. Transgenic mice were identified by both PCR and Southern blot analysis of genomic DNA prepared from the tail. The sets of primers used to identify the transgenic animals are listed in **Supplementary Table 8** online. For transgene analysis, 10 μg of genomic DNA were digested with BamHI and size fractionated on a 1% agarose gel in 1× TAE. The Southern blots were hybridized with [^{32}P]-labeled genomic probes (570 bp) containing *MSMG01-414M07* sequences.

TST and FST. After weaning, mice of the same sex were maintained in a group (1–5 mice per cage) under an LD 12:12 cycle (7:00 on, 19:00 off) at approximately 24 °C with food and water *ad libitum* in our animal facility. Before the TST and FST, these mice were moved to the animal room adjacent to the test room where their behaviors were assayed, and the mice were kept there for 1 week under the same conditions as those before moving. We assayed mice aged 8–12 weeks during the light (11:00–16:00) after at least a 2-h adaptation to the test room. The procedure for TST was based on a previous study[2], but with slight modifications[40]. In our test, the mice were suspended by their tails using an elastic band (5 cm in diameter) attached to the tail by adhesive tape (approximately 1 cm from the tip of the tail), and the elastic band was hooked on a horizontal rod. The distance between the tip of the nose of the mouse and the floor was approximately 20 cm. The mice were suspended for a period of 7 min, and the time spent immobile during the last 6 min of 7 min was scored for each individual by an observer blinded to the genotype.

On day 2 after the TST, the pre-session of the FST was performed. We placed the mice in plastic cylinders (height, 30 cm; diameter, 20 cm) containing water (25 ± 1 °C; depth, 15 cm) for 15 min. On the next day, we placed the mice in the same cylinder and scored the time immobile during the last 6 min of the 7 min of forced swimming[22,41].

© 2009 Nature America, Inc. All rights reserved.

In the TST, we examined the effects of administration of imipramine (Wako) on the immobility time. The mice were intraperitoneally injected with 10 ml kg^{-1} of the vehicle (saline) or imipramine (5 mg kg^{-1}) and subjected to the TST at 40 min after injection.

Muscimol-induced righting reflex. Mice were subcutaneously injected with muscimol (Bachem, 3 mg kg^{-1}) dissolved in saline and placed on their backs into a V-shaped trough every 10 min after the injection to measure the latency until the return of the righting reflex. The loss of the righting reflex was defined as the inability of the mouse to right itself within 30 s. The recovery of the righting reflex was determined when a mouse righted twice in the 2 consecutive 30-s trials.

Nest building. Approximately 1 h before the dark phase of LD 12:12, we placed the mice individually in a cage with wood-chip bedding and one nestlet made of pressed cotton (Lillico; 2.5 g, 5 cm × 5 cm). Based on a previous report[42], the nests were assessed on the next morning using the following rating scale: 1, >90% intact; 2, 50–90% intact; 3, 10–50% intact; 4, 0–10% intact, but flat nest; 5, 0–10% intact, with walls higher than the height of the mouse. The amount of nest material was measured by subtracting the weight of the untorn nestlet pieces (loose material and bedding were brushed off) from the total weight.

Open-field test. Each mouse was placed in the center of a gray plastic box (40 × 40 × 40 cm) with the floor divided into 64 compartments (5 × 5 cm each) and was allowed to freely explore for 5 min under 40-lx to 50-lx fluorescent light. The test was conducted during the light phase of LD 12:12 (11:00–16:00). During the test, the number of boundaries of the compartment passed, grooming, rearing and defecation were scored.

Light-dark box test. The light-dark box consisted of a dark and a light compartment (each compartment: width, 15 cm; height, 15 cm; length, 25 cm) that were divided by a partition with a small opening (width, 42 mm; height, 44 mm) through which the mice could move between the compartments. The dark and light compartments were made of black and clear plexiglas, respectively. During the light phase of LD 12:12 (11:00–16:00), each mouse was placed in the center of the light compartment and allowed to freely explore the box for 5 min under 40-lx to 50-lx fluorescent light. The inside of the dark compartment was not illuminated. The observer scored the number of light-dark transitions between the two compartments, the total time spent in the dark compartment and the number of episodes of defecation[41].

Elevated plus-maze test. The elevated plus-maze consists of two open arms (width, 8 cm; length, 25 cm) and two closed arms (width, 8 cm; height, 20 cm; length, 25 cm) that extend from a common central platform (8 × 8 cm)[41,43]. This apparatus was elevated to a height of 50 cm above the floor. Each mouse was placed on the center square, facing an open arm, and was allowed to freely explore for 5 min under 40-lx to 50-lx fluorescent light. We scored the number of open and closed arm entries, the total time spent on the open arm and the number of episodes of defecation. We conducted this test during the light phase of LD 12:12 (11:00–16:00).

Y-maze test. We examined short-term memory by the Y-maze test based on the method reported previously[22]. The Y-maze was made of wood that had been painted black, and each arm was 40 cm long, 12 cm high, 3 cm wide at the bottom and 10 cm wide at the top. The arms converged at a central equilateral triangular area with its longest axis measuring 4 cm. The apparatus was placed on the floor of the experimental room and was illuminated with a 100 W bulb placed 200 cm above. Each mouse was placed at the end of one arm and allowed to move freely through the maze during an 8-min session, and the series of arm entries was recorded visually. The alternation behavior was defined by successive entries into the three arms, on overlapping triplet sets, and such behavior (%) was expressed as the ratio of actual alternations (defined as the total number of arm entries minus two), multiplied by 100. After the experiments, we counted the number of arm entries.

Prepulse inhibition test. The apparatus used and the procedure were the same as reported previously[44]. The startle chambers (SR-LAB; San Diego Instruments) consisted of nonrestrictive plexiglas cylinders, 3.8 cm in diameter and 13 cm long, resting on a plexiglas platform in a ventilated and well-lit chamber connected with a measurement cage containing a signal amplification sensor. A high-frequency speaker mounted 33 cm above the cylinder produced all acoustic stimuli. A piezoelectric accelerometer was mounted under each cylinder and detected transduced animal movements. A computer and interface assembly digitized and stored the data. A dynamic calibration system (SR-LAB; San Diego Instruments) was used to ensure comparable sensitivities across the chambers. The sound levels were measured in decibels. The background white noise was 70 dB in the soundproof box of the loudspeaker as measured from the upper part of the measurement cage.

Six different trial types were presented in the test session: 40-ms broadband 87-dB (prepulse-alone trial) and 118-dB (pulse-alone trial) bursts; three different prepulse (pp) + pulse (p) trials in which 40-ms-long 10-dB (pp10p118), 13-dB (pp13p118) or 17-dB (pp17p118) stimuli above a 70-dB background white noise preceded the 118-dB pulse by 100 ms (onset to onset); and a no-stimulus trial, in which only the background white noise was presented[44]. Thus, the six trial types presented were pulse alone, prepulse alone, pp10p118, pp13p118, pp17p118 and no stimulus. Each of the six different trial types was presented in a random order eight times. The intertrial interval was 30 s. The test session consisted of 48 trials. The session began with a 5-min acclimatization period followed by test session. The vibration was examined 100 ms after auditory stimulation (pulse) as the startle amplitude. The prepulse inhibition was obtained as follows: prepulse inhibition = ((pulse-alone response × (prepulse + pulse response))/(pulse-alone response)) × 100.

Hole board test. The hole board test consisted of a 40-cm square plane with 16 flush-mounted cylindrical holes (each measuring 3 cm in diameter) distributed 4 × 4 in an equidistant, grid-like manner[45]. The mice were placed one by one at the center of the board and were allowed to move about freely for a period of 5 min each under 40 lx to 50 lx. During the test (the light phase of LD 12:12, 11:00–16:00), the number of head dips (defined as placing the head into a hole) was counted.

Electrophysiology. Hippocampal slices (250 μm thick) were obtained from the B/B, C/C and C/C tg strain aged P33–P41 as described previously[46]. Whole-cell patch-clamp recordings were performed from hippocampal CA1 pyramidal neurons using an EPC9/2 amplifier (HEKA Electronik) and a PowerLab (ADI Instruments) with infrared-differential interference contrast visualization. Patch pipettes (3–5 MΩ) were filled with a solution containing (in mM) 124 Cs-methanesulfonate, 11 KCl, 2 $MgCl_2$, 0.1 EGTA, 10 HEPES, 4 Na_2-ATP, 0.3 GTP, 5 QX-314 and 0.5% biocytin (brought to pH 7.3 with CsOH, osmolarity 280 mOsm). The liquid junction potential of the solution was 9.65 mV and corrected. $GABA_A$ receptor–mediated current was recorded as an outward current at a holding potential of 0 mV in the presence of the NMDA receptor antagonist D-(−)-2-amino-5-phosphonopentanoic acid (AP5; 25 μM), the AMPA receptor antagonist 6-cyano-7-nitroquinoxaline-2,3-dione (CNQX; 10 μM) and tetrodotoxin (TTX; 0.5 μM). Muscimol was bath-applied for 2.5 min to the same cells recorded at increasing concentrations of 0.1, 1.0 and 10.0 μM, and the maximum current at each concentration was measured as the muscimol current at each concentration. Miniature inhibitory synaptic currents (mIPSCs) were analyzed offline with MiniAnalysis 6.0.7 (Synaptosoft). The detection threshold of miniature currents was set at twice the baseline noise.

Immunohistochemistry. Immunohistochemistry was performed as previously described[47] with minor modifications. We fixed brains with 4% paraformaldehyde in phosphate-buffered saline (PBS) and obtained hippocampal slices (20-μm thick) with a cryostat (MICROM HM560; MICRO EDGE) according to a previously described atlas[48]. Fluorescent images were captured directly in some samples, and images were acquired with a confocal microscope (LSM510; Carl Zeiss) or a light microscope (AxioCam HRc; Carl Zeiss). Monoclonal mouse anti-GAD67 (1:100, Millipore Corporation) diluted in PBS containing 0.01% Triton X-100 and 5% rabbit serum was applied to sections, which were then incubated overnight at 4 °C. After washing by 0.01% Triton X-100 in PBS, rabbit anti-mouse Alexa Fluor 488 (1:1000, Invitrogen) was added to sections as a fluorescently conjugated secondary antibody for 2 h at room temperature (approximately 20 °C). Every fourth, fifth and sixth section throughout the hippocampus (total 12 sections) was processed for GAD67 immnohistochemistry. To quantify the immunoreactivities of GAD67, we used the imaging software WinRoof (Mitani Co. Ltd.)[47,49]. The areas of GAD67-positive cells mm^{-2} were measured in the hippocampus. The average of the three determinations for each mouse was used for statistical analysis.

© 2009 Nature America, Inc. All rights reserved.

Statistics. The results are represented as the mean ± s.e.m. One-way ANOVA using a Tukey-Kramer *post hoc* test, Student's *t*-test with Bonferroni correction or two-way ANOVA was used for comparison among multiple datasets; Student's *t*-test or Mann-Whitney *U* test was used for comparison between two groups.

Note: Supplementary information is available on the Nature Genetics website.

ACKNOWLEDGMENTS

We thank the late M. Ukai (Meijo University) for his helpful suggestions and for providing the facilities for the behavioral experiments, A. Yoshiki (RIKEN BRC) for his useful suggestions regarding the rescue experiment with transgenic mice, S. Yasuo (Johann Wolfgang Goethe-University Frankfurt) for her guidance on the *in situ* hybridization experiment, RIKEN BRC for providing the mice and the Nagoya University Radio-isotope Center for allowing us to use their facilities. This research was supported in part by a Grant-in-Aid for Scientific Research to S.E. and by the Academic Frontier Project for Private Universities (2007–2011) from the Ministry of Education, Culture, Sports, Science and Technology of Japan to T.M and T.N.

AUTHOR CONTRIBUTIONS

S.E. designed the experiments, supervised the project and prepared the manuscript. S.T. designed and performed most of the experiments, analyzed the data and prepared the manuscript. H.S. performed the behavioral tests. T.M. and T.K. supervised the behavioral experiments. T.N. organized GABA-related experiments, and M.Mi, T.A. and M.Ma. performed electrophysiological experiments. M.N. contributed to histological examination. J.K., S.I. and A.I. conducted the QTL analysis. K.A. supervised the production of BAC transgenic mice. Y.I. and S.I. contributed to congenic strain breeding and phenotyping. T.Y. provided the facilities and provided technical support.

Published online at http://www.nature.com/naturegenetics/
Reprints and permissions information is available online at http://npg.nature.com/reprintsandpermissions/

© 2009 Nature America, Inc. All rights reserved.

1. Porsolt, R.D., Lepichon, M. & Jalfre, M. Depression—new animal-model sensitive to antidepressant treatments. *Nature* **266**, 730–732 (1977).
2. Steru, L., Chermat, R., Thierry, B. & Simon, P. The tail suspension test—a new method for screening antidepressants in mice. *Psychopharmacology (Berl.)* **85**, 367–370 (1985).
3. Cryan, J.F. & Mombereau, C. In search of a depressed mouse: utility of models for studying depression-related behavior in genetically modified mice. *Mol. Psychiatry* **9**, 326–357 (2004).
4. Cryan, J.F., Mombereau, C. & Vassout, A. The tail suspension test as a model for assessing antidepressant activity: review of pharmacological and genetic studies in mice. *Neurosci. Biobehav. Rev.* **29**, 571–625 (2005).
5. Watanabe, A. *et al.* Fabp7 maps to a quantitative trait locus for a schizophrenia endophenotype. *PLoS Biol.* **5**, e297 (2007).
6. Flint, J., Valdar, W., Shifman, S. & Mott, R. Strategies for mapping and cloning quantitative trait genes in rodents. *Nat. Rev. Genet.* **6**, 271–286 (2005).
7. Turri, M.G., Datta, S.R., DeFries, J., Henderson, N.D. & Flint, J. QTL analysis identifies multiple behavioral dimensions in ethological tests of anxiety in laboratory mice. *Curr. Biol.* **11**, 725–734 (2001).
8. Yoshikawa, T., Watanabe, A., Ishitsuka, Y., Nakaya, A. & Nakatani, N. Identification of multiple genetic loci linked to the propensity for "behavioral despair" in mice. *Genome Res.* **12**, 357–366 (2002).
9. Crowley, J.J., Brodkin, E.S., Blendy, J.A., Berrettini, W.H. & Lucki, I. Pharmacogenomic evaluation of the antidepressant citalopram in the mouse tail suspension test. *Neuropsychopharmacology* **31**, 2433–2442 (2006).
10. Liu, X., Stancliffe, D., Lee, S., Mathur, S. & Gershenfeld, H.K. Genetic dissection of the tail suspension test: a mouse model of stress vulnerability and antidepressant response. *Biol. Psychiatry* **62**, 81–91 (2007).
11. Lad, H.V., Liu, L., Paya-Cano, J.L., Fernandes, C. & Schalkwyk, L.C. Quantitative traits for the tail suspension test: automation, optimization, and BXD RI mapping. *Mamm. Genome* **18**, 482–491 (2007).
12. Suzuki, T. *et al.* Quantitative trait locus analysis of abnormal circadian period in CS mice. *Mamm. Genome* **12**, 272–277 (2001).
13. Abe, H., Honma, S., Honma, K., Suzuki, T. & Ebihara, S. Functional diversities of two activity components of circadian rhythm in genetical splitting mice (CS strain). *J. Comp. Physiol. [A]* **184**, 243–251 (1999).
14. Abe, H., Honma, S. & Honma, K. Daily restricted feeding resets the circadian clock in the suprachiasmatic nucleus of CS mice. *Am. J. Physiol. Regul. Integr. Comp. Physiol.* **292**, R607–R615 (2007).
15. Ebihara, S., Miyazaki, S., Sakamaki, H. & Yoshimura, T. Sleep properties of CS mice with spontaneous rhythm splitting in constant darkness. *Brain Res.* **980**, 121–127 (2003).
16. Belknap, J.K. *et al.* QTL analysis and genomewide mutagenesis in mice: complementary genetic approaches to the dissection of complex traits. *Behav. Genet.* **31**, 5–15 (2001).
17. Flint, J. & Mott, R. Finding the molecular basis of quantitative traits: successes and pitfalls. *Nat. Rev. Genet.* **2**, 437–445 (2001).
18. Crawley, J.N. Behavioral phenotyping of transgenic and knockout mice: experimental design and evaluation of general health, sensory functions, motor abilities, and specific behavioral tests. *Brain Res.* **835**, 18–26 (1999).
19. Bourin, M. & Hascoet, M. The mouse light/dark box test. *Eur. J. Pharmacol.* **463**, 55–65 (2003).
20. Karl, T., Pabst, R. & von Horsten, S. Behavioral phenotyping of mice in pharmacological and toxicological research. *Exp. Toxicol. Pathol.* **55**, 69–83 (2003).
21. Braff, D.L., Geyer, M.A. & Swerdlow, N.R. Human studies of prepulse inhibition of startle: normal subjects, patient groups, and pharmacological studies. *Psychopharmacology (Berl.)* **156**, 234–258 (2001).
22. Mamiya, T. *et al.* Effects of pre-germinated brown rice on beta-amyloid protein-induced learning and memory deficits in mice. *Biol. Pharm. Bull.* **27**, 1041–1045 (2004).
23. Chattopadhyaya, B. *et al.* GAD67-mediated GABA synthesis and signaling regulate inhibitory synaptic innervation in the visual cortex. *Neuron* **54**, 889–903 (2007).
24. Solberg, L.C. *et al.* Sex- and lineage-specific inheritance of depression-like behavior in the rat. *Mamm. Genome* **15**, 648–662 (2004).
25. Amerik, A.Y. & Hochstrasser, M. Mechanism and function of deubiquitinating enzymes. *Biochim. Biophys. Acta* **1695**, 189–207 (2004).
26. Nijman, S.M. *et al.* A genomic and functional inventory of deubiquitinating enzymes. *Cell* **123**, 773–786 (2005).
27. Liu, G.X. *et al.* Reduced anxiety and depression-like behaviors in mice lacking GABA transporter subtype 1. *Neuropsychopharmacology* **32**, 1531–1539 (2007).
28. DeLorey, T.M., Sahbaie, P., Hashemi, E., Homanics, G.E. & Clark, J.D. Gabrb3 gene deficient mice exhibit impaired social and exploratory behaviors, deficits in non-selective attention and hypoplasia of cerebellar vermal lobules: a potential model of autism spectrum disorder. *Behav. Brain Res.* **187**, 207–220 (2008).
29. Maguire, J. & Mody, I. GABA(A)R plasticity during pregnancy: relevance to postpartum depression. *Neuron* **59**, 207–213 (2008).
30. Korn, H. & Faber, D.S. Quantal analysis and synaptic efficacy in the CNS. *Trends Neurosci.* **14**, 439–445 (1991).
31. Liang, J. *et al.* Mechanisms of reversible GABAA receptor plasticity after ethanol intoxication. *J. Neurosci.* **27**, 12367–12377 (2007).
32. Meier, E., Belhage, E., Drejer, J. & Schousboe, A. The expression of GABA receptors on cultured cerebellar granule cells is influenced by GABA. in *Neurotrophic Activity of GABA During Development* (eds. Redburn, D.A. & Shousboe, A.) 139–159 (Alan R. Liss, Inc., New York,, 1987).
33. Owens, D.F. & Kriegstein, A.R. Is there more to GABA than synaptic inhibition? *Nat. Rev. Neurosci.* **3**, 715–727 (2002).
34. Churchill, G.A. & Doerge, R.W. Empirical threshold values for quantitative trait mapping. *Genetics* **138**, 963–971 (1994).
35. Broman, K.W., Wu, H., Sen, S. & Churchill, G.A. R/qtl: QTL mapping in experimental crosses. *Bioinformatics* **19**, 889–890 (2003).
36. Ishikawa, A., Hatada, S., Nagamine, Y. & Namikawa, T. Further mapping of quantitative trait loci for postnatal growth in an inter-sub-specific backcross of wild *Mus musculus* castaneus and C57BL/6J mice. *Genet. Res.* **85**, 127–137 (2005).
37. Markel, P. *et al.* Theoretical and empirical issues for marker-assisted breeding of congenic mouse strains. *Nat. Genet.* **17**, 280–284 (1997).
38. Yoshimura, T. *et al.* Molecular analysis of avian circadian clock genes. *Brain Res. Mol. Brain Res.* **78**, 207–215 (2000).
39. Abe, K. *et al.* Contribution of Asian mouse subspecies *Mus musculus* molossinus to genomic constitution of strain C57BL/6J, as defined by BAC-end sequence-SNP analysis. *Genome Res.* **14**, 2439–2447 (2004).
40. Ukai, M., Maeda, H., Nanya, Y., Kameyama, T. & Matsuno, K. Beneficial effects of acute and repeated administrations of sigma receptor agonists on behavioral despair in mice exposed to tail suspension. *Pharmacol. Biochem. Behav.* **61**, 247–252 (1998).
41. Miyamoto, Y. *et al.* Lower sensitivity to stress and altered monoaminergic neuronal function in mice lacking the NMDA receptor epsilon 4 subunit. *J. Neurosci.* **22**, 2335–2342 (2002).
42. Deacon, R.M. Assessing nest building in mice. *Nat. Protoc.* **1**, 1117–1119 (2006).
43. Mamiya, T., Noda, Y., Nishi, M., Takeshima, H. & Nabeshima, T. Enhancement of spatial attention in nociceptin/orphanin FQ receptor-knockout mice. *Brain Res.* **783**, 236–240 (1998).
44. Ukai, M., Okuda, A. & Mamiya, T. Effects of anticholinergic drugs selective for muscarinic receptor subtypes on prepulse inhibition in mice. *Eur. J. Pharmacol.* **492**, 183–187 (2004).
45. Ghelardini, C. *et al.* Antisense knockdown of the Shaker-like Kv1.1 gene abolishes the central stimulatory effects of amphetamines in mice and rats. *Neuropsychopharmacology* **28**, 1096–1105 (2003).
46. Miura, M., Saino-Saito, S., Masuda, M., Kobayashi, K. & Aosaki, T. Compartment-specific modulation of GABAergic synaptic transmission by mu-opioid receptor in the mouse striatum with green fluorescent protein-expressing dopamine islands. *J. Neurosci.* **27**, 9721–9728 (2007).
47. Niwa, M. *et al.* A novel molecule "shati" is involved in methamphetamine-induced hyperlocomotion, sensitization, and conditioned place preference. *J. Neurosci.* **27**, 7604–7615 (2007).
48. Franklin, K.B.J. & Paxinos, G. *The Mouse Brain: in Stereotaxic Coordinates* (Academic Press, San Diego, 1997).
49. Kuwahara, M., Sugimoto, M., Tsuji, S., Miyata, S. & Yoshioka, A. Cytosolic calcium changes in a process of platelet adhesion and cohesion on a von Willebrand factor-coated surface under flow conditions. *Blood* **94**, 1149–1155 (1999).

Please cite this article in press as: Niwa et al., Knockdown of DISC1 by In Utero Gene Transfer Disturbs Postnatal Dopaminergic Maturation in the Frontal Cortex and Leads to Adult Behavioral Deficits, Neuron (2010), doi:10.1016/j.neuron.2010.01.019

Neuron
Article

別刷 No.13

Knockdown of DISC1 by In Utero Gene Transfer Disturbs Postnatal Dopaminergic Maturation in the Frontal Cortex and Leads to Adult Behavioral Deficits

Minae Niwa,[1,2,3,11] Atsushi Kamiya,[1,11] Rina Murai,[2,4] Ken-ichiro Kubo,[5] Aaron J. Gruber,[6] Kenji Tomita,[5] Lingling Lu,[2] Shuta Tomisato,[7] Hanna Jaaro-Peled,[1] Saurav Seshadri,[1] Hideki Hiyama,[1] Beverly Huang,[1] Kazuhisa Kohda,[7] Yukihiro Noda,[8] Patricio O'Donnell,[6] Kazunori Nakajima,[5] Akira Sawa,[1,9,*] and Toshitaka Nabeshima[2,4,10,*]

[1]Department of Psychiatry and Behavioral Sciences, Johns Hopkins University School of Medicine, Baltimore, MD 21287, USA
[2]Department of Chemical Pharmacology, Meijo University, Nagoya 4688503, Japan
[3]Department of Psychiatry
[4]Department of Neuropsychopharmacology and Hospital Pharmacy
Nagoya University Graduate School of Medicine, Nagoya 4668560, Japan
[5]Department of Anatomy, Keio University School of Medicine, Tokyo 1608582, Japan
[6]Department of Anatomy and Neurobiology, University of Maryland School of Medicine, Baltimore, MD 21201, USA
[7]Department of Physiology, Keio University School of Medicine, Tokyo 1608582, Japan
[8]Division of Clinical Science and Neuropsychopharmacology, Meijo University, Nagoya 4688503, Japan
[9]Department of Neuroscience, Johns Hopkins University School of Medicine, Baltimore, MD 21287, USA
[10]The Academic Frontier Project for Private Universities, Comparative Cognitive Science Institutes, Nagoya 4688503, Japan
[11]These authors contributed equally to this work
*Correspondence: asawa1@jhmi.edu (A.S.), tnabeshi@ccmfs.meijo-u.ac.jp (T.N.)
DOI 10.1016/j.neuron.2010.01.019

SUMMARY

Adult brain function and behavior are influenced by neuronal network formation during development. Genetic susceptibility factors for adult psychiatric illnesses, such as Neuregulin-1 and Disrupted-in-Schizophrenia-1 (DISC1), influence adult high brain functions, including cognition and information processing. These factors have roles during neurodevelopment and are likely to cooperate, forming pathways or "signalosomes." Here we report the potential to generate an animal model via in utero gene transfer in order to address an important question of how nonlethal deficits in early development may affect postnatal brain maturation and high brain functions in adulthood, which are impaired in various psychiatric illnesses such as schizophrenia. We show that transient knockdown of DISC1 in the pre- and perinatal stages, specifically in a lineage of pyramidal neurons mainly in the prefrontal cortex, leads to selective abnormalities in postnatal mesocortical dopaminergic maturation and behavioral abnormalities associated with disturbed cortical neurocircuitry after puberty.

INTRODUCTION

Adult brain function and behavior are influenced by neuronal network formation during development. Consequently, disturbances of brain development are suggested to underlie the pathology of adult mental disorders, such as schizophrenia and mood disorders (Lewis and Levitt, 2002; Rapoport et al., 2005; Savitz and Drevets, 2009; Tenyi et al., 2009). Consistent with this notion, genetic susceptibility factors for these disorders that have been recently identified, including Neuregulin-1 and Disrupted-in-Schizophrenia-1 (DISC1), have roles during neurodevelopment and are likely to cooperate, forming molecular "pathways" (Harrison and Weinberger, 2005; Jaaro-Peled et al., 2009; Owen et al., 2005). Furthermore, many studies have indicated that variations of these disease susceptibility genes influence high brain functions, including cognition and information processing, in both normal subjects and patients (Kéri, 2009; Krug et al., 2008; Tomppo et al., 2009). Thus, these genetic factors are believed to be good probes to explore mechanistic links between brain development and adult brain functions.

Schizophrenia is a debilitating disorder with onset in young adulthood, although many lines of evidence have indicated that pre- and perinatal brain disturbances underlie the initial risks for the disease (Buka and Fan, 1999; McNeil, 1995). It is possible that these initial risks may in turn affect postnatal brain maturation, resulting in the delayed onset of the disorder. Prodromal stages of schizophrenia in adolescence and young adulthood may reflect the dynamic pathophysiology of disturbed brain maturation (Cannon et al., 2003; Jaaro-Peled et al., 2009; White et al., 2006). Some excellent longitudinal studies with clinical subjects have attempted to address this question (White et al., 2006). Nonetheless, good animal models that can depict the sequential changes from the initial disturbances in early brain development to defects of postnatal brain maturation, leading to adult brain dysfunction associated with schizophrenia, are awaited to permit dissection and understanding of the molecular mechanisms during the course of disease progression. Mice with manipulations of genetic susceptibility factors for the disease may provide this opportunity (Chen et al., 2006). Once available, such models may shed light on the pathological

Please cite this article in press as: Niwa et al., Knockdown of DISC1 by In Utero Gene Transfer Disturbs Postnatal Dopaminergic Maturation in the Frontal Cortex and Leads to Adult Behavioral Deficits, Neuron (2010), doi:10.1016/j.neuron.2010.01.019

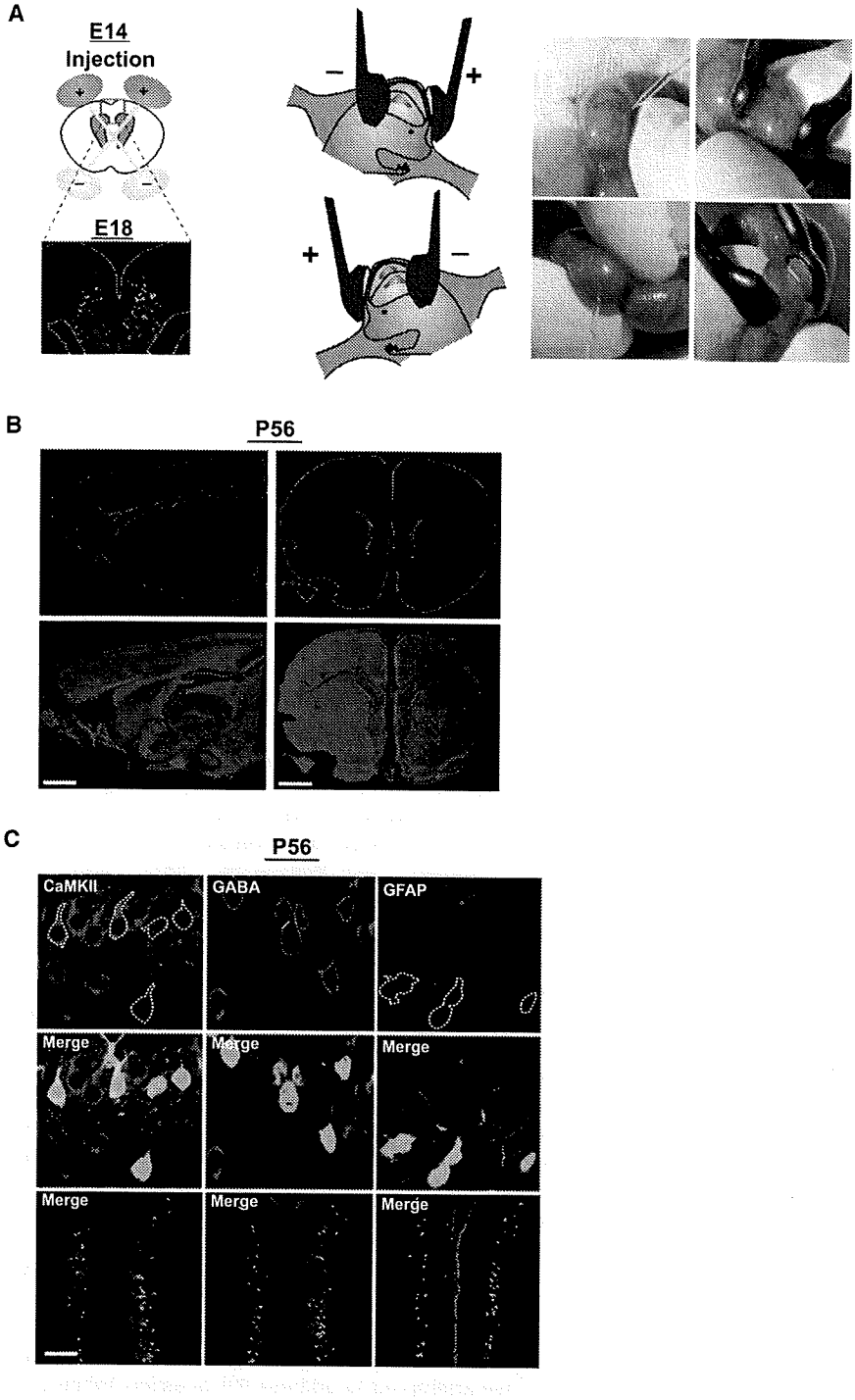

Figure 1. Selective Targeting of Constructs to Cells in a Lineage of Pyramidal Neurons in the Prefrontal Cortex via In Utero Gene Transfer

(A) Schematic representation of bilateral in utero injection of constructs followed by their incorporation by electroporation into progenitor cells in the ventricular zone at embryonic day 14 (E14). Migrating cells with GFP are visualized at E18 after injection of a GFP expression construct.

(B) Representative coronal and sagittal images of brains with GFP expression at P56 after injection of a GFP expression construct at E14. Blue, nucleus. The scale bars represent 1 mm.

(C) GFP-positive neurons in layers II/III at postnatal day 56 (P56) in mPFC. Most cells with GFP expression are CaMKII-positive pyramidal neurons (red in left panels), but not GABA (red in middle panels) or GFAP positive (red in right panels) at P56. The scale bar represents 100 μm.

mechanisms for schizophrenia. Furthermore, even more importantly, these models may clarify how minor or nonlethal brain disturbances in early development, possibly related to a combination of genetic variations, may affect high brain functions in adults, including cognition and information processing, in a wide range of mental conditions and even in subjects who may not be classified as having psychiatric disorders as defined by the Diagnostic and Statistical Manual of Mental Disorders.

Here we provide evidence to support the feasibility of in utero gene transfer to produce mouse models to address this question. In the present study, by utilizing this technique, we generated mice in which selective knockdown of DISC1 is achieved in a lineage for pyramidal neurons mainly in the prefrontal cortex (PFC), but only during development, which leads to maturation-dependent deficits in mesocortical dopaminergic projections and associated behavioral changes, including those in information processing and cognition.

RESULTS

Application of In Utero Gene Transfer to Modulate Expression of Target Genes in the Prefrontal Cortex

To evaluate the feasibility of the in utero gene transfer technique to analyze the modulation of gene expression in the PFC, an expression construct of green fluorescent protein (GFP) was injected into bilateral lateral ventricles and incorporated by electroporation into progenitor cells in the ventricular zone at embryonic day 14 (E14) in mice (Figure 1A; see Figure S1A available online). We analyzed sagittal and serial coronal sections from six randomly selected brains at postnatal day 56 (P56), and found that GFP-positive cells were located at +2.34 mm to ~+0.98 mm relative to Bregma, especially in the dorsolateral prefrontal cortex (DLPFC), medial prefrontal cortex (mPFC), orbitofrontal cortex (OFC), and anterior cingulate cortex (Figures 1B, S1B, and S1C). Thus, this method allows for gene targeting mainly into

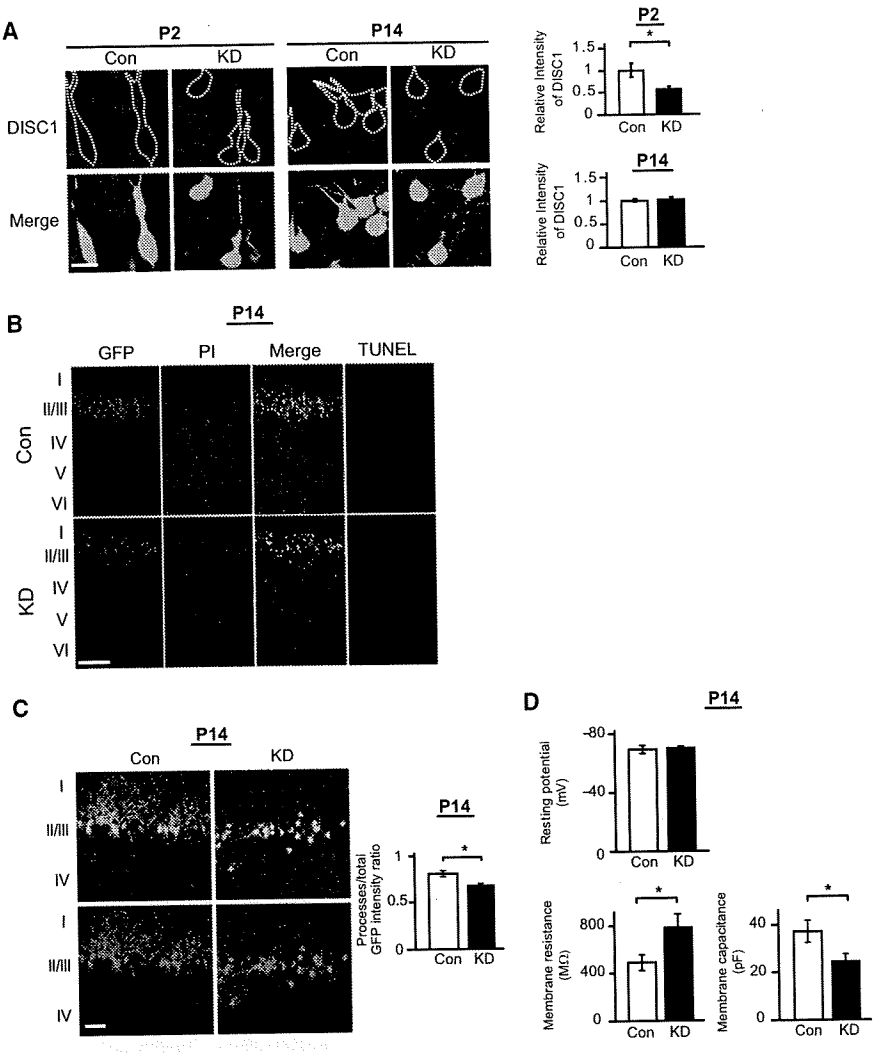

Figure 2. Mice with Knockdown of DISC1 in Pyramidal Neurons of the Prefrontal Cortex during Early Development via In Utero Gene Transfer Display Dendritic Abnormalities at P14

(A) Suppression of DISC1 immunoreactivity (red) in GFP-positive neurons is observed at P2, but not at P14, when shRNA to DISC1 is introduced (DISC1 knockdown [KD]) at E14 (*$p < 0.05$). A total of 30 GFP-positive cells from cortical slices of three DISC1 KD mice and those of three control mice with scrambled/control shRNA was analyzed and compared. The scale bar represents 10 μm.

(B) GFP-positive neurons with RNAi at layers II/III at P14 after injection at E14. KD mice display dendritic pathology without signs of apoptosis (TUNEL), consistent with our previous publication (Kamiya et al., 2005). Red, nucleus. The scale bar represents 100 μm.

(C) Reduction of GFP fluorescence intensity in dendrites relative to total GFP fluorescence intensity in mPFC of KD mice at P14, compared to those of Con mice (*$p < 0.05$, $n = 5$ per condition), suggesting impaired dendritic formation in KD mice. Red, nucleus. The scale bar represents 50 μm.

(D) Electrophysiological characteristics of pyramidal neurons with knockdown of DISC1 (majority of green cells) at layers II/III in mPFC at P14. Membrane resistance at −80 mV and membrane capacitance of GFP-positive neurons in DISC1 KD mice are significantly different compared with those in Con mice (*$p < 0.05$), whereas there is no difference in resting potential in these two groups ($n = 5$ per condition).

Data are expressed as mean ± SEM.

the PFC. In the developing cerebral cortex, pyramidal neurons migrate radially from the ventricular zone, whereas interneurons migrate tangentially from ganglionic eminence into the developing cerebral wall (Anderson et al., 1997; Marin and Rubenstein, 2003). Glial lineages originating from the subventricular zone are produced at late embryonic and early postnatal days (E17 to P14) (Sauvageot and Stiles, 2002). Therefore, the constructs are likely to be integrated into cells in a lineage of pyramidal neurons. Indeed, GFP-positive cells were confined only to pyramidal neurons, around 20% of which were GFP positive in layers II/III at P56 (Figure 1C). These results indicate that in utero gene transfer can be used for modulating target gene expression mainly in pyramidal neurons in PFC during brain development.

Transient Knockdown of DISC1 in PFC during Development via In Utero RNAi Transfer

In this study, we used DISC1 as a probe to address how molecular disturbance in cells of the pyramidal neuron lineage in PFC during early development might influence postnatal brain maturation and adult phenotypes. Thus, we injected a well-characterized DISC1 short-hairpin RNA (shRNA) together with a GFP expression construct at E14 according to the protocol described above, and confirmed targeting to PFC. Histological phenotypes in the developing cortex elicited by this shRNA (defects in neuronal progenitor proliferation, delay in neuronal migration, and resultant changes in arborization) are consistent with those elicited by other shRNAs to DISC1 thus far reported (Kamiya et al., 2005; Mao et al., 2009), and are rescued by overexpression of wild-type DISC1 ($DISC1^R$) (Figure S2A). Suppression of DISC1 seems to be transient, confirmed by knockdown of DISC1 for at least 7 days after injection, but not after 3 weeks (Figure 2A). In the present study, we have characterized the DISC1 knockdown-elicited phenotypic changes at P14 in greater detail, by extending our previous observation (Kamiya et al., 2005). As the result of the transient knockdown of DISC1 via RNA interference (RNAi) (designated DISC1 KD in this manuscript), GFP-positive pyramidal neurons were found in layers II/III without signs of apoptosis and with abnormal dendritic morphology (Figures 2B, 2C, and S2B–S2D). Impaired dendritic development in layers II/III at P14 in DISC1 KD mice was also functionally confirmed by electrophysiological approaches (Figure 2D).

Please cite this article in press as: Niwa et al., Knockdown of DISC1 by In Utero Gene Transfer Disturbs Postnatal Dopaminergic Maturation in the Frontal Cortex and Leads to Adult Behavioral Deficits, Neuron (2010), doi:10.1016/j.neuron.2010.01.019

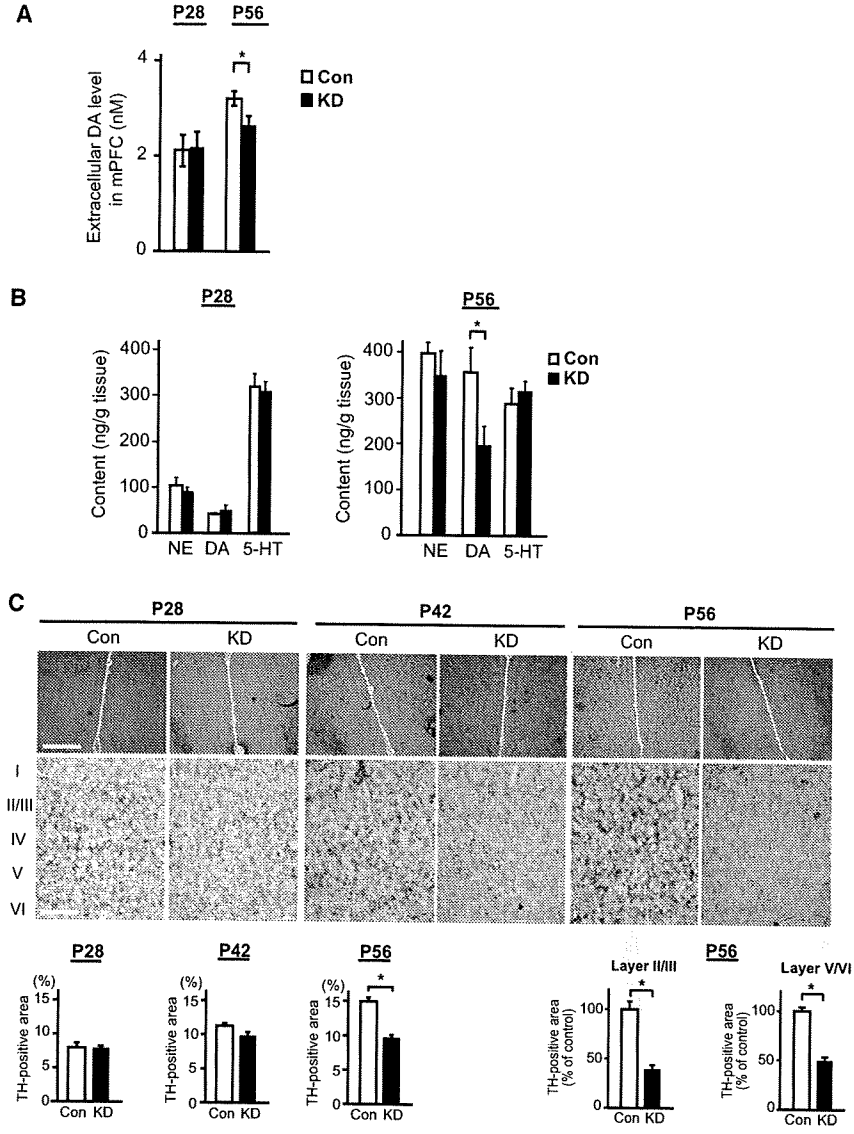

Figure 3. Disturbance in Postnatal Maturation of Mesocortical Dopaminergic Projections to the Medial Prefrontal Cortex in DISC1 Knockdown Mice

(A) Basal levels of extracellular dopamine (DA) in mPFC were analyzed by in vivo microdialysis, and a decrease in DISC1 KD mice compared with that in Con mice was detected at P56, but not at P28 (*$p < 0.05$, $n = 6$ per condition).

(B) Monoamine content in the frontal cortex as measured by HPLC. The level of DA in FC is decreased in DISC1 KD mice compared with that in Con mice at P56, but not at P28 (*$p < 0.05$, $n = 7$ per condition). No difference in the levels of NE and 5-HT is observed at these two time points.

(C) Immunostaining of tyrosine hydroxylase (TH) in mPFC, including prelimbic and infralimbic cortex (upper panels, low magnification; bottom panels, high magnification). TH level in mPFC is relatively decreased in KD mice compared with Con mice at P56 (*$p < 0.05$, $n = 6$ per condition) in both layers II/III and V/VI, whereas there is no difference between KD and Con at P28 and P42. The scale bar in low-magnification pictures represents 200 μm, and in high-magnification pictures represents 500 μm.

Data are expressed as mean ± SEM.

Disturbance in Postnatal Maturation of Mesocortical Dopaminergic Projections and Interneurons to the Medial Prefrontal Cortex in DISC1 KD Mice

Next, we addressed whether the dendritic abnormalities at P14 elicited by transient knockdown of DISC1 in the pre-/perinatal stages may later influence postnatal brain maturation. We first examined differences in body weight between DISC1 KD and control mice at P14, P28, and P56, which may reflect atypical developmental trajectories and could potentially affect maturation of neuronal circuits and behavior nonspecifically, but no difference in body weight was observed between these two groups (Figure S3A). At the histological level, we did not find any robust differences in Nissl staining in mPFC at P28 and P56 (Figure S3B). No difference between DISC1 KD and controls in immunostaining and western blotting for glial fibrillary acidic protein (GFAP) indicated that there was no gliosis in DISC1 KD mice at P28 and P56 (Figures S3C and S3D).

In contrast, we observed a marked decrease in the extracellular levels of dopamine in mPFC, measured by microdialysis, and total content of dopamine between KD and controls in FC at P56 but not at P28 (Figures 3A and 3B), whereas no changes were observed in total content of dopamine in other brain areas including nucleus accumbens, hippocampus, and cerebellum (Figure S3E). This change may be specific to dopamine, as no changes in glutamate, norepinephrine (NE), or serotonin were observed (Figure 3B, S3E, and S3F). Increase in the level of dopamine from birth to adolescence in the frontal cortex is known to reflect physiological maturation of the dopaminergic projection (Benes et al., 2000; Goto and Grace, 2007; Rosenberg and Lewis, 1995). Insufficient elevation of dopamine at P56 in DISC1 KD mice may indicate disturbed maturation of dopaminergic neurons. Consistent with this idea, relative immunoreactivity against tyrosine hydroxylase (TH), a marker of mature axon terminals of the dopaminergic projection, was decreased in both layers II/III and V/VI at P56, but not at P28 and P42, in DISC1 KD compared to control mice (Figure 3C). This relative decrease of TH was also confirmed by western blotting (Figure S3G). In contrast, we did not observe changes in expression of dopamine receptor-1 (D1R) and -2 (D2R) (Figures S3G and S3H).

Given that there are inter- and intralaminar connections of pyramidal neurons and GABAergic interneurons in local circuits in PFC where mesocortical dopaminergic neurons also have synaptic contact (Sesack et al., 2003), this aberrant development

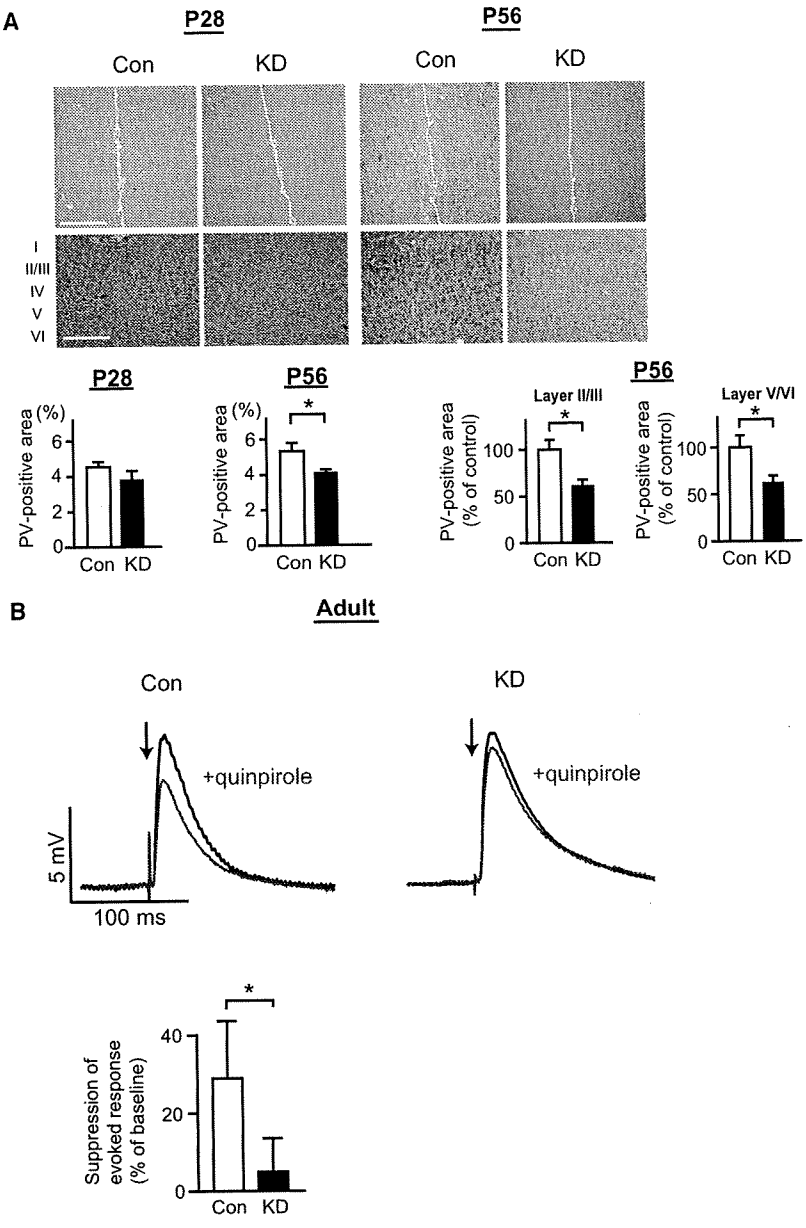

Figure 4. Disturbances of Interneurons and Pyramidal Neurons in PFC of DISC1 KD Mice after Puberty

(A) Immunostaining of parvalbumin (PV) in the mPFC (upper panels, low magnification; bottom panels, high magnification). Immunoreactivity of PV is quantified under each condition (lower graphs). The expression levels of PV in the mPFC (both layers II/III and V/VI) are decreased in KD mice compared with Con mice at P56, but not at P28 (*$p < 0.05$, $n = 6$ per condition). The scale bar in low-magnification pictures represents 200 μm, and in high-magnification pictures represents 500 μm.

(B) Electrophysiological responses of PFC pyramidal neurons to electrical stimulation recorded using the whole-cell patch-clamp technique in acute slices from young adult male mice. Overlay of membrane potential responses evoked with electrical stimulation of cortico-cortical fibers before (black trace) and during (red trace) bath application of the D2 dopamine agonist quinpirole (5 μM) in KD and Con mice. Arrows indicate times of single-pulse stimulation. Quinpirole attenuation of evoked excitatory postsynaptic potentials is reduced in KD mice (*$p < 0.05$, $n = 5$ per condition).

Data are expressed as mean ± SEM.

of the pyramidal neurons may affect GABAergic interneurons. To test this possibility, we examined the expression level of parvalbumin, a marker of the fast-spiking GABAergic interneurons. We observed reduction of parvalbumin immunoreactivity in layers II/III and V/VI in mPFC in DISC1 KD mice at P56 but not at P28, suggesting that there is a possible deficit of interneurons in adulthood; this effect is likely to occur during postnatal brain maturation (Figure 4A). To test whether dopamine regulation of local circuit processing in mPFC is altered in adult DISC1 KD mice, we recorded deep-layer pyramidal neurons by using the whole-cell patch-clamp technique in acute brain slices (Figure S4). Neither resting membrane potential nor input resistance was different from controls, indicating that basic somatic electrophysiological properties are not grossly disrupted in adult DISC1 KD mice (data not shown). Nonetheless, bath application of the D2R dopamine receptor agonist quinpirole attenuated electrically evoked membrane responses in control mice, but such attenuation was markedly reduced in DISC1 KD mice (Figure 4B). Taken together, these results suggest that neonatal pyramidal neuron deficits elicited by pre-/perinatal knockdown of DISC1 lead to overall disturbances in circuitry involving dopamine neurons, pyramidal neurons, and interneurons, manifested only after puberty.

Behavioral Deficits in DISC1 KD Mice after Puberty

We then questioned whether such neurochemical and physiological disturbance in postnatal brain maturation might result in behavioral deficits. Prepulse inhibition (PPI) reflects sensory gating function, a major indicator of information processing involving the cortex, which is also frequently impaired in various mental illnesses (Arguello and Gogos, 2006). DISC1 KD mice at P56, but not at P28, displayed decreased PPI, in comparison with controls (Figure 5A). DISC1-associated PPI deficits are further confirmed in mice by another shRNA to DISC1 that knocks down this molecule to a lesser extent than does the shRNA mainly used in this study (Kamiya et al., 2005, 2008; Mao et al., 2009): milder deficits in PPI that were consistent with the milder effect on DISC1 expression were observed in the mice (Figure S5A). We also tested the effect of clozapine, which is reported to elevate dopamine levels via blocking the D2 autoreceptor (Rayevsky et al., 1995). Very interestingly, when we administered clozapine acutely to DISC1 KD mice, we observed

Please cite this article in press as: Niwa et al., Knockdown of DISC1 by In Utero Gene Transfer Disturbs Postnatal Dopaminergic Maturation in the Frontal Cortex and Leads to Adult Behavioral Deficits, Neuron (2010), doi:10.1016/j.neuron.2010.01.019

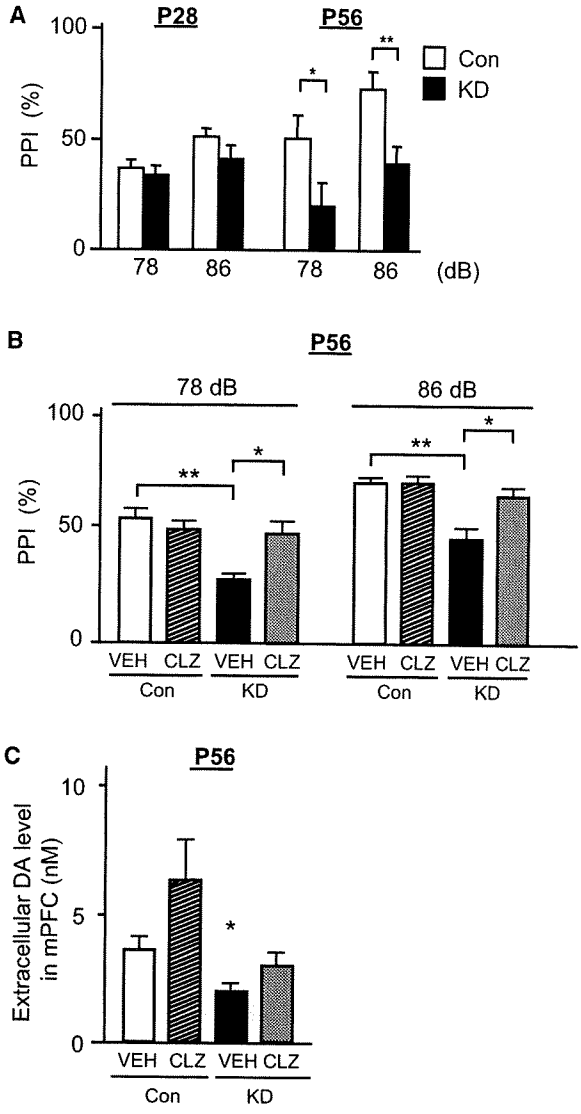

Figure 5. Attenuation of Prepulse Inhibition Deficits by Treatment with Clozapine in DISC1 KD Mice after Puberty

(A) Performance in prepulse inhibition (PPI) at P28 and P56. Impairment of PPI is observed in DISC1 KD mice at P56, but not at P28 (*$p < 0.05$, **$p < 0.01$, $n = 12$ per condition).

(B) Effect of clozapine (CLZ) on the impairment of PPI in KD mice at P56. Treatment with CLZ (3 mg/kg, i.p.) ameliorates the impairment of PPI in KD mice at P56 (*$p < 0.05$, **$p < 0.01$, $n = 16$ per condition). VEH, vehicle.

(C) Effect of CLZ on extracellular DA levels in mPFC by in vivo microdialysis. Administration of CLZ (3 mg/kg, i.p.) elevates extracellular DA levels in mPFC in both Con and KD mice at P56 (*$p < 0.05$, $n = 4$ per condition).

Data are expressed as mean ± SEM.

normalized levels of dopamine in mPFC and improvement of PPI deficits, without alterations in the startle amplitude (Figures 5B, 5C, S5B, and S5C). These results suggest that PPI deficits in DISC1 KD mice are, at least in part, associated with decreased levels of dopamine in the mPFC at P56.

The novel object recognition task (NORT) measures functions of the hippocampus and the cortex, including functions associated with visual working memory (Ozawa et al., 2006). No difference was observed in exploratory preference during the training between control and KD mice, suggesting that there were no significant differences in curiosity and/or motivation to explore objects between the two groups (Figure S5D). In contrast, KD mice at P56, but not at P28, displayed impaired performance in the test runs 24 hr after the training session, whereas no difference was found 1 hr after the training session (Figures S5D and S5E). Acute administration of clozapine improved their performance in NORT (Figure S5F). To address a function more specific to the cortex, mice were assessed by a T maze test at P56. DISC1 KD mice showed significantly fewer correct choices than did control mice, with delay intervals of 15 s, although there was no difference in required training time between the two groups (Figure S5G). In contrast, no difference was observed between DISC1 KD and control mice in the forced-swim test, a paradigm associated with depression (Figure S5H).

Next, in order to examine dopamine-associated behavioral deficits in DISC1 KD mice further, we challenged DISC1 KD mice with the psychostimulant methamphetamine. Although DISC1 KD mice did not differ from controls in spontaneous locomotion in the open field (Figure S6), DISC1 KD mice at P56, but not at P28, displayed hypersensitivity to administration of methamphetamine in locomotion (Figure 6A). Consistent with this result, we found that the increase of extracellular dopamine levels in nucleus accumbens in DISC1 KD mice was higher than that in controls after the administration of methamphetamine, although the basal levels of extracellular dopamine were slightly lower in DISC1 KD mice than in controls (Figure 6B).

DISCUSSION

There are two major conclusions in the present study. First, we report the potential to generate an animal model via in utero gene transfer in order to address an important question of how nonlethal deficits in early development may affect postnatal brain maturation of information processing and cognition in adulthood. Second, we show that transient knockdown of DISC1 in the pre- and perinatal stages, specifically in a lineage of pyramidal neurons mainly in PFC, leads to abnormalities in postnatal mesocortical dopaminergic maturation which results in overall disturbance in circuitry and several behavioral abnormalities in adulthood. Although there is precedence that insults in early development lead to delayed phenotypic manifestations in rodents (Koshibu et al., 2005; Lipska et al., 1993; Moore et al., 2006), the present study indicates the sequential link among pre-/perinatal disturbance in a specific genetic susceptibility factor (DISC1), the associated dendritic abnormalities in the neonatal stage, and, in turn, selective phenotypes in adolescence and adulthood.

This study may aid molecular understanding of how initial insults during early development disturb postnatal brain maturation for many years which results in full-blown onset of schizophrenia after puberty (Buka and Fan, 1999; Jaaro-Peled et al., 2009; McNeil, 1995). Although it is still being debated, brains from patients with schizophrenia show abnormalities in the cortex, especially in layers II/III, which include decreased arborization and smaller size of pyramidal neurons, as well as alteration

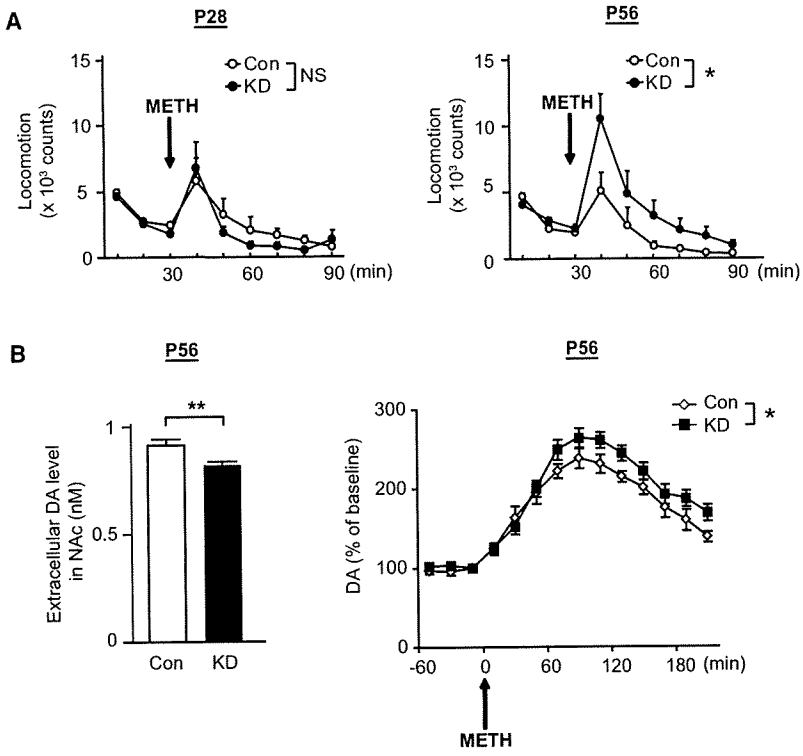

Figure 6. Hypersensitivity to the Psychostimulant Methamphetamine in DISC1 KD Mice after Puberty

(A) Methamphetamine (METH; 1 mg/kg, s.c.) -induced hyperactivity is augmented in DISC1 KD mice compared with Con mice, at P56 but not at P28 (*$p < 0.05$, $n = 6–10$ per condition).

(B) The extent of increase after METH challenge in levels of extracellular DA relative to those at the baseline is augmented in the nucleus accumbens (NAc) of DISC1 KD mice compared with Con mice at P56 (*$p < 0.05$, $n = 8$ per condition) (right), whereas mild but significant reduction of basal levels of extracellular DA is observed in KD mice (**$p < 0.01$, $n = 8$ per condition) (left).

Data are expressed as mean ± SEM.

in a subset of interneurons (Akbarian et al., 1995; Benes and Berretta, 2001; Glantz and Lewis, 2000; Guidotti et al., 2000; Lewis et al., 2005; Selemon and Goldman-Rakic, 1999). Furthermore, a decrease in tyrosine hydroxylase staining in schizophrenia patients has been reported, suggesting a reduction of dopaminergic innervation in the prefrontal cortex in schizophrenia (Akil et al., 1999). Primary defects for these cytoarchitectural changes may occur during neurodevelopment, because they are not accompanied by gliosis. Nevertheless, it has been unclear what kinds of neurodevelopmental defects result in such brain anatomical changes in patients with schizophrenia, with clinical onset 15–30 years after birth, characterized by psychosis and impaired cognition and information processing, and associated with aberrant neurotransmission, especially dopaminergic neurotransmission. The model in this study represents a majority of these objective characteristics reported in schizophrenia research. Therefore, to address the hierarchy and mechanistic links of these characteristics, this DISC1 model produced via in utero gene transfer may be useful. For example, an important question for future mechanistic studies with this model is how a decrease in tyrosine hydroxylase in all layers, or disturbance of postnatal maturation of mesocortical dopaminergic projections, is induced by dendritic abnormalities of the pyramidal neurons in layer II/III in the cortex in early development. Another question is how dysfunction of mesocortical dopaminergic projection affects its mesolimbic circuitry, including possible changes in dynamics of dopamine uptake and release, in the nucleus accumbens.

Although various types of genetically engineered animals, including inducible and conditional systems, have been developed, the in utero gene transfer technique with expression and/or shRNA constructs for RNAi may be a promising alternative methodology. We can select the target cell populations for genetic modulation specifically, by changing the direction of the electroporation (LoTurco et al., 2009). Thus, preferential targeting to a lineage of interneurons in the cortex or to hippocampal neurons is also technically feasible by targeting the electrodes toward ganglionic eminence or medial regions of the embryonic telencephalon, respectively (Borrell et al., 2005; Navarro-Quiroga et al., 2007). Furthermore, introduction of inducible expression constructs in in utero gene transfer will allow us to have better control of target gene expression (LoTurco et al., 2009; Manent et al., 2009; Matsuda and Cepko, 2007).

Many investigators have considered the possibility that adult brain function and behavior are influenced by neuronal network formation during development (Cannon et al., 2003; Harrison and Weinberger, 2005; Jaaro-Peled et al., 2009; Lisman et al., 2008), which is modulated by a combination of several genetic and environmental factors, and the concept of "pathway(s)" is more likely to mimic the mechanisms than the effect of a single gene product. By using the technical advantage of in utero transfer in which expression of more than one gene can be modified at one time by cotransfection of expression and/or RNAi constructs (Kamiya et al., 2008; Shu et al., 2004; Tsai et al., 2005; Young-Pearse et al., 2007), we will be able to test the synergistic influence or epistatic effect of multiple genetic factors. In a more general application, we propose that this method is useful in testing how modest but significant defects in neuronal network formation in early development lead to adult behavioral traits; furthermore, if potential variation between batches and animals is well controlled, this technique may also be utilized in trying to build novel animal models for various adult mental disorders, including schizophrenia, in which multiple risk factors play etiological roles during neurodevelopment.

EXPERIMENTAL PROCEDURES

Constructs

Short-hairpin RNA (shRNA) to DISC1 (5′-GGCAAACACTGTGAAGTGC-3′) was expressed by an H1 promoter-driven pSuper plasmid (Brummelkamp et al.,

Please cite this article in press as: Niwa et al., Knockdown of DISC1 by In Utero Gene Transfer Disturbs Postnatal Dopaminergic Maturation in the Frontal Cortex and Leads to Adult Behavioral Deficits, Neuron (2010), doi:10.1016/j.neuron.2010.01.019

2002). This shRNA was shown to effectively knock down DISC1 in cell cultures and in vivo via in utero gene transfer in previous publications from more than one research group (Kamiya et al., 2005, 2008; Mao et al., 2009). The duration of knockdown expression of genes by this H1-driven pSuper plasmid is dependent on the target molecules that we have tested so far (data not shown), and suppression of DISC1 was clearly transient in the developing cortex. Scrambled target sequence without homology to any known messenger RNA was used to produce the control RNAi. The expression construct used for rescue control experiments ($DISC1^R$) is described in Supplemental Information. The GFP expression construct is under the control of the CAG promoter.

In Utero Electroporation

In utero electroporation was performed by our published protocol with some modifications (Kamiya et al., 2005; Tabata and Nakajima, 2001). We used ICR mice, because neuropathological changes induced by the same shRNA to DISC1 had been characterized in this strain (Kamiya et al., 2005, 2008). Pregnant mice were anesthetized at E14 by intraperitoneal administration of 2,2,2-tribromoethanol in tert-amyl alcohol (0.4 mg/g). Two centimeter midline laparotomy was performed and the uterine horn was exposed. RNAi plasmids (2 μg/μl) together with GFP expression vector with CAG promoter (1 μg/μl) (molar ratio approximately 3:1) were injected into the bilateral ventricles with a glass micropipette made from a microcapillary tube (GD-1; Narishige). Injected plasmid solution contained Fast Green solution (0.001%) to monitor the injection. The embryo's head in the uterus was held between the tweezers-type electrode consisting of two disc electrodes of 5 mm diameter (CUY650-5; Tokiwa Science). Depending on which hemisphere was injected, the electrodes were oriented at a rough 20° outward angle from the midline and a rough 30° angle downward from an imaginary line from the olfactory bulbs to the caudal side of the cortical hemisphere. Electrode pulses (35V; 50 ms) were charged five times at intervals of 950 ms with an electroporator (CUY21E; Tokiwa Science). The uterine horn was placed back into the abdominal cavity and the abdominal wall and skin were sutured. All experiments were performed in accordance with the institutional guidelines for animal experiments.

Histology and Quantitative Analyses

Histological procedures were performed as previously described (Kamiya et al., 2005) with minor modifications. Brains were fixed with 4% paraformaldehyde, and coronal sections, including mPFC, were obtained with a cryostat at 20 μm (CM 1850; Leica). For immunohistochemistry, the following primary antibodies were used: anti-DISC1 (1: 100) (Ozeki et al., 2003), anti-tyrosine hydroxylase (TH) (1:100; Millipore), anti-parvalbumin (PV) (1:100; Sigma-Aldrich), anti-CaMKII (1:200; Upstate Biotechnology), and anti-GABA (1:200; Sigma-Aldrich). Fluorescent secondary antibodies conjugated to Alexa 488 and Alexa 568 (Molecular Probes) as well as biotin-conjugated secondaries were used for chromogen detection. Nuclei were labeled with Neurotrace Nissl 530/615 (Molecular Probes), propidium iodide (Molecular Probes), or DAPI (Molecular Probes). TUNEL staining was carried out as published (Yu et al., 2003).

To evaluate which types of cells were targeted by in utero gene transfer, the number of double-labeled cells with GFP together with specific cell markers, such as CaMKII (for pyramidal neurons), GABA (for interneurons), and GFAP (for astrocytes), was counted in a region of interest defined as 100 μm wide × 50 μm high in layers II/III in mPFC. Two regions of interest were randomly selected from three mice (a total of six regions). Images were acquired with a confocal microscope (LSM510; Carl Zeiss). The ratio of the number of double-labeled cells to that of cells with each cell marker was measured.

In order to quantify the effect of RNAi on expression of DISC1, the immunofluorescent intensity of DISC1 signal in each GFP-positive cell was measured by using MetaMorph software version 7.1 (MDS Analytical Technologies) after images were acquired with a confocal microscope (LSM510). The acquisition parameters were kept the same for all images. The intensity of the signal from randomly selected 10 GFP-positive cells in layers II/III of mPFC was quantitatively assessed in three DISC1 KD and three Con mice (i.e., 30 cells from DISC1 KD and 30 cells from Con mice). The signal in a region of equal size without cells in the lateral ventricle was subtracted as background.

To quantify immunoreactivity of TH and PV, a region of interest was defined as 800 μm wide × 1300 μm high in mPFC in the coronal sections (anteroposterior [AP]: +1.98 to +1.54 mm; mediolateral (ML): ± 0.8 mm from Bregma; dorsoventral [DV]: −1.75 to −3.05 mm from the dura) according to the atlas of Franklin and Paxinos (2007). Three images were acquired with a light microscope (Axioskop2 plus; Carl Zeiss) for each brain (six brains per DISC1 KD and control mice). The acquisition parameters were kept the same for all images. The areas of TH- or PV-positive cells/mm^2 were measured by the imaging software WinRoof (Mitani) after subtraction of the threshold value. The threshold was automatically measured at a minimum level by this software in the first image from a control mouse sample at P28 and was kept constant across all images.

For the procedures of morphological analysis of dendrites, see Supplemental Experimental Procedures.

Microdialysis

Microdialysis was carried out as previously described (Niwa et al., 2007) with a minor modification. A guide cannula (AG-6; Eicom) was implanted into the mPFC (15° angle from AP: +1.7 mm; ML: −1.0 mm from Bregma; DV: −1.5 mm from the dura) or nucleus accumbens (AP: +1.7 mm; ML: −0.8 mm from Bregma; DV: −4.0 mm from the dura). Ringer's solution (147 mM NaCl, 4 mM KCl, and 2.3 mM $CaCl_2$) was continuously perfused (1.0 μl/min). The dialysates were collected every 10 min and analyzed by high-performance liquid chromatography (HPLC) (Eicom). The levels of dopamine were also analyzed after the intraperitoneal injection of clozapine (3 mg/kg) (Sigma-Aldrich) or subcutaneous injection of methamphetamine (METH) (1 mg/kg) (Dainippon Sumitomo).

High-Performance Liquid Chromatography

Brains were removed rapidly, and each brain region was dissected out on ice according to the atlas of Franklin and Paxinos (2007). The brain homogenates were centrifuged at 20,000 × *g* for 15 min at 4°C, and the supernatants were mixed with 1 M sodium acetate to adjust to pH 3.0 for analysis by HPLC and by electrochemical detector (Eicom). The contents of norepinephrine (NE), dopamine (DA), and 5-hydroxytryptamine (5-HT) were determined as previously described (Miyamoto et al., 2002).

Electrophysiology

Mice were perfused with ice-cold artificial cerebrospinal fluid (ACSF) containing 125 mM NaCl, 25 mM $NaHCO_3$, 10 mM glucose, 3.5 mM KCl, 1.25 mM NaH_2PO_4, 0.5 mM (for P14) or 0.1 mM (for adult stage) $CaCl_2$, and 3 mM $MgCl_2$ (pH 7.4); osmolarity 285–295 mOsm. Coronal slices of brains at 400 μm (AP: +1.7 to 2.1 mm from Bregma) were made on a Vibratome and incubated in ACSF solution (35°C) oxygenated with 95% O_2 and 5% CO_2 for 60–70 min. For the recording ACSF, $CaCl_2$ was increased to 2 mM and $MgCl_2$ was decreased to 1 mM. All experiments were conducted at 33°C–35°C.

At P14, whole-cell recordings were performed from the GFP-labeled pyramidal neurons in layers II/III in the mPFC. Patch pipettes (3–6 MΩ) were filled with 115 mM K gluconate, 20 mM KCl, 10 mM KOH, 2 mM $MgCl_2$, 4 mM Na_2ATP, 1 mM NaGTP, 10 mM HEPES, 0.4 mM EGTA (pH 7.2). The τ_m was obtained by single-exponential fitting and the membrane capacitance was calculated.

At adult stage, whole-cell recordings were performed from pyramidal neurons in layers V/VI in the mPFC, where GFP-labeled cells were located in layers II/III, and identified under visual guidance by using infrared differential interference contrast video microscopy. Electrical stimulation (1 pulse, 0.2–1.4 mA) was applied through an electrode consisting of tungsten wire. The stimulating electrode was placed near layer I, 0.7–1 mm lateral to the location of whole-cell recordings in layers V/VI . Patch pipettes (9–12 MΩ) were filled with 115 mM K gluconate, 10 mM HEPES, 2 mM $MgCl_2$, 20 mM KCl, 2 mM MgATP, 2 mM Na_2ATP, and 0.3 mM GTP (pH 7.3); 285–295 mOsm. All bath-applied drugs, such as quinpirole and CNQX, were applied in the recording solution at known concentrations. Single pulses of current were delivered every 20 s, and stimulation current was adjusted so as to produce 4–10 mV postsynaptic potentials with reliable amplitude. Baseline responses to stimulation were recorded prior to adding quinpirole (5 μM) for 5–6 min. The magnitude of evoked responses was averaged over the baseline and compared to

the average during the 5 min time interval from +2 to +7 min after quinpirole addition. This period was chosen for consistency, with differences revealed by previous investigations of D2 modulation of PFC activity in rodent models of schizophrenia (Tseng et al., 2008).

Behavioral Analysis

Prepulse Inhibition

Prepulse inhibition (Arguello and Gogos, 2006) of the acoustic startle response was measured using an SR-LAB System (San Diego Instruments). The stimulus onset consisted of a 20 ms prepulse, a 100 ms delay, and then a 40 ms startle pulse. The intensity of the prepulse was 8 or 16 dB above the 70 dB background noise. The amount of prepulse inhibition was calculated as a percentage of the 120 dB acoustic startle response: 100 – [(startle reactivity on prepulse + startle pulse)/startle reactivity on startle pulse] × 100. PPI tests were also performed 30 min after the intraperitoneal injection of clozapine (3 mg/kg).

Locomotor Activity

To measure spontaneous activity, mice were placed in a transparent acrylic cage, and locomotion and rearing were measured every 5 min for 60 min by using digital counters with infrared sensors (Scanet SV-10; Merquest) as described previously (Miyamoto et al., 2002). To measure methamphetamine (METH) -induced hyperactivity, mice received one subcutaneous injection of METH (1 mg/kg) after 30 min of prehabituation in a cage (Miyamoto et al., 2004).

Unbiased Assessment in Experimental Procedures

To avoid experimental bias by investigators, in utero surgery and all analyses, including those for DISC1 immunostaining and behavioral tests, were conducted by multiple investigators in a systematic manner as follows: an investigator conducted in utero surgery without knowing the identification of constructs. Furthermore, investigators conducted several assays without knowing the identification of mice (either DISC1 KD or controls).

Statistical Analysis

The Student's *t* test was used in comparing two sets of data. Statistical differences among more than three groups were determined using one-way analysis of variance (ANOVA), two-way ANOVA, or ANOVA with repeated measures followed by Bonferroni multiple comparison tests. A value of $p < 0.05$ was considered statistically significant. All data are expressed as mean ± SEM.

SUPPLEMENTAL INFORMATION

Supplemental Information includes six figures and Supplemental Experimental Procedures and can be found with this article online at doi:10.1016/j.neuron.2010.01.019.

ACKNOWLEDGMENTS

We thank Dr. Pamela Talalay and Dr. Eva Anton for critical reading and Ms. Yukiko Lema for organizing the manuscript. This work was supported by U.S. Public Heath Service grant MH-069853 (A.S.), Silvio O. Conte Center grants MH-084018 (A.S.) and MH-088753 (A.S.), and foundation grants from Stanley (A.S.), S-R (A.S., A.K.), RUSK (A.S.), and NARSAD (A.S., A.K., H.J.-P.). This work was also supported by grants from JSPS (T.N., K.N., M.N.), MEXT (T.N., K.N.), MARC (T.N.), MHLW (T.N., K.K.), Sumitomo (K.N.), Naito (K.N.), Academic Frontier Project (T.N.), and Takeda (T.N., K.N.).

Accepted: January 14, 2010
Published: February 24, 2010

REFERENCES

Akbarian, S., Kim, J.J., Potkin, S.G., Hagman, J.O., Tafazzoli, A., Bunney, W.E., Jr., and Jones, E.G. (1995). Gene expression for glutamic acid decarboxylase is reduced without loss of neurons in prefrontal cortex of schizophrenics. Arch. Gen. Psychiatry *52*, 258–266.

Akil, M., Pierri, J.N., Whitehead, R.E., Edgar, C.L., Mohila, C., Sampson, A.R., and Lewis, D.A. (1999). Lamina-specific alterations in the dopamine innervation of the prefrontal cortex in schizophrenic subjects. Am. J. Psychiatry *156*, 1580–1589.

Anderson, S.A., Eisenstat, D.D., Shi, L., and Rubenstein, J.L. (1997). Interneuron migration from basal forebrain to neocortex: dependence on Dlx genes. Science *278*, 474–476.

Arguello, P.A., and Gogos, J.A. (2006). Modeling madness in mice: one piece at a time. Neuron *52*, 179–196.

Benes, F.M., and Berretta, S. (2001). GABAergic interneurons: implications for understanding schizophrenia and bipolar disorder. Neuropsychopharmacology *25*, 1–27.

Benes, F.M., Taylor, J.B., and Cunningham, M.C. (2000). Convergence and plasticity of monoaminergic systems in the medial prefrontal cortex during the postnatal period: implications for the development of psychopathology. Cereb. Cortex *10*, 1014–1027.

Borrell, V., Yoshimura, Y., and Callaway, E.M. (2005). Targeted gene delivery to telencephalic inhibitory neurons by directional in utero electroporation. J. Neurosci. Methods *143*, 151–158.

Brummelkamp, T.R., Bernards, R., and Agami, R. (2002). A system for stable expression of short interfering RNAs in mammalian cells. Science *296*, 550–553.

Buka, S.L., and Fan, A.P. (1999). Association of prenatal and perinatal complications with subsequent bipolar disorder and schizophrenia. Schizophr. Res. *39*, 113–119.

Cannon, T.D., van Erp, T.G., Bearden, C.E., Loewy, R., Thompson, P., Toga, A.W., Huttunen, M.O., Keshavan, M.S., Seidman, L.J., and Tsuang, M.T. (2003). Early and late neurodevelopmental influences in the prodrome to schizophrenia: contributions of genes, environment, and their interactions. Schizophr. Bull. *29*, 653–669.

Chen, J., Lipska, B.K., and Weinberger, D.R. (2006). Genetic mouse models of schizophrenia: from hypothesis-based to susceptibility gene-based models. Biol. Psychiatry *59*, 1180–1188.

Franklin, B.J.K., and Paxinos, G. (2007). The Mouse Brain in Stereotaxic Coordinates (San Diego: Academic Press).

Glantz, L.A., and Lewis, D.A. (2000). Decreased dendritic spine density on prefrontal cortical pyramidal neurons in schizophrenia. Arch. Gen. Psychiatry *57*, 65–73.

Goto, Y., and Grace, A.A. (2007). The dopamine system and the pathophysiology of schizophrenia: a basic science perspective. Int. Rev. Neurobiol. *78C*, 41–68.

Guidotti, A., Auta, J., Davis, J.M., Di-Giorgi-Gerevini, V., Dwivedi, Y., Grayson, D.R., Impagnatiello, F., Pandey, G., Pesold, C., Sharma, R., et al. (2000). Decrease in reelin and glutamic acid decarboxylase67 (GAD67) expression in schizophrenia and bipolar disorder: a postmortem brain study. Arch. Gen. Psychiatry *57*, 1061–1069.

Harrison, P.J., and Weinberger, D.R. (2005). Schizophrenia genes, gene expression, and neuropathology: on the matter of their convergence. Mol. Psychiatry *10*, 40–68.

Jaaro-Peled, H., Hayashi-Takagi, A., Seshadri, S., Kamiya, A., Brandon, N.J., and Sawa, A. (2009). Neurodevelopmental mechanisms of schizophrenia: understanding disturbed postnatal brain maturation through neuregulin-1-ErbB4 and DISC1. Trends Neurosci. *32*, 485–495.

Kamiya, A., Kubo, K., Tomoda, T., Takaki, M., Youn, R., Ozeki, Y., Sawamura, N., Park, U., Kudo, C., Okawa, M., et al. (2005). A schizophrenia-associated mutation of DISC1 perturbs cerebral cortex development. Nat. Cell Biol. *7*, 1167–1178.

Kamiya, A., Tan, P.L., Kubo, K., Engelhard, C., Ishizuka, K., Kubo, A., Tsukita, S., Pulver, A.E., Nakajima, K., Cascella, N.G., et al. (2008). Recruitment of PCM1 to the centrosome by the cooperative action of DISC1 and BBS4: a candidate for psychiatric illnesses. Arch. Gen. Psychiatry *65*, 996–1006.

Kéri, S. (2009). Genes for psychosis and creativity: a promoter polymorphism of the neuregulin 1 gene is related to creativity in people with high intellectual achievement. Psychol. Sci. *20*, 1070–1073.

Koshibu, K., Ahrens, E.T., and Levitt, P. (2005). Postpubertal sex differentiation of forebrain structures and functions depend on transforming growth factor-α. J. Neurosci. *25*, 3870–3880.

Krug, A., Markov, V., Leube, D., Zerres, K., Eggermann, T., Nothen, M.M., Skowronek, M.H., Rietschel, M., and Kircher, T. (2008). Genetic variation in the schizophrenia-risk gene neuregulin1 correlates with personality traits in healthy individuals. Eur. Psychiatry *23*, 344–349.

Lewis, D.A., and Levitt, P. (2002). Schizophrenia as a disorder of neurodevelopment. Annu. Rev. Neurosci. *25*, 409–432.

Lewis, D.A., Hashimoto, T., and Volk, D.W. (2005). Cortical inhibitory neurons and schizophrenia. Nat. Rev. Neurosci. *6*, 312–324.

Lipska, B.K., Jaskiw, G.E., and Weinberger, D.R. (1993). Postpubertal emergence of hyperresponsiveness to stress and to amphetamine after neonatal excitotoxic hippocampal damage: a potential animal model of schizophrenia. Neuropsychopharmacology *9*, 67–75.

Lisman, J.E., Coyle, J.T., Green, R.W., Javitt, D.C., Benes, F.M., Heckers, S., and Grace, A.A. (2008). Circuit-based framework for understanding neurotransmitter and risk gene interactions in schizophrenia. Trends Neurosci. *31*, 234–242.

LoTurco, J., Manent, J.B., and Sidiqi, F. (2009). New and improved tools for in utero electroporation studies of developing cerebral cortex. Cereb. Cortex *19* (*Suppl 1*), i120–i125.

Manent, J.B., Wang, Y., Chang, Y., Paramasivam, M., and LoTurco, J.J. (2009). Dcx reexpression reduces subcortical band heterotopia and seizure threshold in an animal model of neuronal migration disorder. Nat. Med. *15*, 84–90.

Mao, Y., Ge, X., Frank, C.L., Madison, J.M., Koehler, A.N., Doud, M.K., Tassa, C., Berry, E.M., Soda, T., Singh, K.K., et al. (2009). Disrupted in schizophrenia 1 regulates neuronal progenitor proliferation via modulation of GSK3β/β-catenin signaling. Cell *136*, 1017–1031.

Marin, O., and Rubenstein, J.L. (2003). Cell migration in the forebrain. Annu. Rev. Neurosci. *26*, 441–483.

Matsuda, T., and Cepko, C.L. (2007). Controlled expression of transgenes introduced by in vivo electroporation. Proc. Natl. Acad. Sci. USA *104*, 1027–1032.

McNeil, T.F. (1995). Perinatal risk factors and schizophrenia: selective review and methodological concerns. Epidemiol. Rev. *17*, 107–112.

Miyamoto, Y., Yamada, K., Noda, Y., Mori, H., Mishina, M., and Nabeshima, T. (2002). Lower sensitivity to stress and altered monoaminergic neuronal function in mice lacking the NMDA receptor ε 4 subunit. J. Neurosci. *22*, 2335–2342.

Miyamoto, Y., Yamada, K., Nagai, T., Mori, H., Mishina, M., Furukawa, H., Noda, Y., and Nabeshima, T. (2004). Behavioural adaptations to addictive drugs in mice lacking the NMDA receptor ε1 subunit. Eur. J. Neurosci. *19*, 151–158.

Moore, H., Jentsch, J.D., Ghajarnia, M., Geyer, M.A., and Grace, A.A. (2006). A neurobehavioral systems analysis of adult rats exposed to methylazoxymethanol acetate on E17: implications for the neuropathology of schizophrenia. Biol. Psychiatry *60*, 253–264.

Navarro-Quiroga, I., Chittajallu, R., Gallo, V., and Haydar, T.F. (2007). Long-term, selective gene expression in developing and adult hippocampal pyramidal neurons using focal in utero electroporation. J. Neurosci. *27*, 5007–5011.

Niwa, M., Nitta, A., Mizoguchi, H., Ito, Y., Noda, Y., Nagai, T., and Nabeshima, T. (2007). A novel molecule "shati" is involved in methamphetamine-induced hyperlocomotion, sensitization, and conditioned place preference. J. Neurosci. *27*, 7604–7615.

Owen, M.J., Craddock, N., and O'Donovan, M.C. (2005). Schizophrenia: genes at last? Trends Genet. *21*, 518–525.

Ozawa, K., Hashimoto, K., Kishimoto, T., Shimizu, E., Ishikura, H., and Iyo, M. (2006). Immune activation during pregnancy in mice leads to dopaminergic hyperfunction and cognitive impairment in the offspring: a neurodevelopmental animal model of schizophrenia. Biol. Psychiatry *59*, 546–554.

Ozeki, Y., Tomoda, T., Kleiderlein, J., Kamiya, A., Bord, L., Fujii, K., Okawa, M., Yamada, N., Hatten, M.E., Snyder, S.H., et al. (2003). Disrupted-in-Schizophrenia-1 (DISC1): mutant truncation prevents binding to NudE-like (NUDEL) and inhibits neurite outgrowth. Proc. Natl. Acad. Sci. USA *100*, 289–294.

Rapoport, J.L., Addington, A.M., Frangou, S., and Psych, M.R. (2005). The neurodevelopmental model of schizophrenia: update 2005. Mol. Psychiatry *10*, 434–449.

Rayevsky, K.S., Gainetdinov, R.R., Grekhova, T.V., and Sotnikova, T.D. (1995). Regulation of dopamine release and metabolism in rat striatum in vivo: effects of dopamine receptor antagonists. Prog. Neuropsychopharmacol. Biol. Psychiatry *19*, 1285–1303.

Rosenberg, D.R., and Lewis, D.A. (1995). Postnatal maturation of the dopaminergic innervation of monkey prefrontal and motor cortices: a tyrosine hydroxylase immunohistochemical analysis. J. Comp. Neurol. *358*, 383–400.

Sauvageot, C.M., and Stiles, C.D. (2002). Molecular mechanisms controlling cortical gliogenesis. Curr. Opin. Neurobiol. *12*, 244–249.

Savitz, J., and Drevets, W.C. (2009). Bipolar and major depressive disorder: neuroimaging the developmental-degenerative divide. Neurosci. Biobehav. Rev. *33*, 699–771.

Selemon, L.D., and Goldman-Rakic, P.S. (1999). The reduced neuropil hypothesis: a circuit based model of schizophrenia. Biol. Psychiatry *45*, 17–25.

Sesack, S.R., Carr, D.B., Omelchenko, N., and Pinto, A. (2003). Anatomical substrates for glutamate-dopamine interactions: evidence for specificity of connections and extrasynaptic actions. Ann. N Y Acad. Sci. *1003*, 36–52.

Shu, T., Ayala, R., Nguyen, M.D., Xie, Z., Gleeson, J.G., and Tsai, L.H. (2004). Ndel1 operates in a common pathway with LIS1 and cytoplasmic dynein to regulate cortical neuronal positioning. Neuron *44*, 263–277.

Tabata, H., and Nakajima, K. (2001). Efficient in utero gene transfer system to the developing mouse brain using electroporation: visualization of neuronal migration in the developing cortex. Neuroscience *103*, 865–872.

Tenyi, T., Trixler, M., and Csabi, G. (2009). Minor physical anomalies in affective disorders. A review of the literature. J. Affect. Disord. *112*, 11–18.

Tomppo, L., Hennah, W., Miettunen, J., Jarvelin, M.R., Veijola, J., Ripatti, S., Lahermo, P., Lichtermann, D., Peltonen, L., and Ekelund, J. (2009). Association of variants in DISC1 with psychosis-related traits in a large population cohort. Arch. Gen. Psychiatry *66*, 134–141.

Tsai, J.W., Chen, Y., Kriegstein, A.R., and Vallee, R.B. (2005). LIS1 RNA interference blocks neural stem cell division, morphogenesis, and motility at multiple stages. J. Cell Biol. *170*, 935–945.

Tseng, K.Y., Lewis, B.L., Hashimoto, T., Sesack, S.R., Kloc, M., Lewis, D.A., and O'Donnell, P. (2008). A neonatal ventral hippocampal lesion causes functional deficits in adult prefrontal cortical interneurons. J. Neurosci. *28*, 12691–12699.

White, T., Anjum, A., and Schulz, S.C. (2006). The schizophrenia prodrome. Am. J. Psychiatry *163*, 376–380.

Young-Pearse, T.L., Bai, J., Chang, R., Zheng, J.B., LoTurco, J.J., and Selkoe, D.J. (2007). A critical function for β-amyloid precursor protein in neuronal migration revealed by in utero RNA interference. J. Neurosci. *27*, 14459–14469.

Yu, Z.X., Li, S.H., Evans, J., Pillarisetti, A., Li, H., and Li, X.J. (2003). Mutant huntingtin causes context-dependent neurodegeneration in mice with Huntington's disease. J. Neurosci. *23*, 2193–2202.

Neuroscience Letters 470 (2010) 134–138

Contents lists available at ScienceDirect

Neuroscience Letters

journal homepage: www.elsevier.com/locate/neulet

Dysfunction of dopamine release in the prefrontal cortex of dysbindin deficient sandy mice: An *in vivo* microdialysis study

Taku Nagai[a,1], Yuko Kitahara[a,1], Anna Shiraki[a], Takao Hikita[b], Shinichiro Taya[b], Kozo Kaibuchi[b,c], Kiyofumi Yamada[a,c,*]

[a] Department of Neuropsychopharmacology and Hospital Pharmacy, Nagoya University Graduate School of Medicine, Nagoya 466-8560, Japan
[b] Department of Cell Pharmacology, Nagoya University Graduate School of Medicine, Nagoya 466-8560, Japan
[c] CREST, JST, Nagoya 466-8560, Japan

ARTICLE INFO

Article history:
Received 19 November 2009
Received in revised form
26 December 2009
Accepted 29 December 2009

Keywords:
Dysbindin
Schizophrenia
Dopamine
Prefrontal cortex
Microdialysis
Mice

ABSTRACT

Dystrobrevin binding protein-1 gene (*DTNBP1*), which encodes dysbindin protein, has been identified as a schizophrenia susceptibility gene. Dysbindin has been shown to contribute to the regulation of exocytosis and formation of synaptic vesicles. Although hypofrontality in schizophrenia underlies its pathophysiology, the molecular function of dysbindin in synaptic neurotransmission remains unclear. In the present study, we investigated depolarization-evoked dopamine (DA) and serotonin (5-HT) release in the prefrontal cortex (PFC) of sandy (sdy) mice, which have a deletion mutation in the gene encoding *DTNBP1*. *In vivo* microdialysis analysis revealed that extracellular DA levels in the PFC of wild-type mice were increased by 60 mM KCl stimulation, and the KCl-evoked DA release was significantly decreased in sdy mice compared with wild-type mice. Extracellular 5-HT levels in the PFC of wild-type mice were also increased by 60 mM KCl stimulation. The KCl-evoked 5-HT release did not differ between wild-type and sdy mice. There was no difference in basal levels of DA and 5-HT before the stimulation between two groups. Behavioral sensitization after repeated methamphetamine (METH) treatment was significantly reduced in sdy mice compared with wild-type mice whereas no difference was observed in METH-induced hyperlocomotion between two groups. These results suggest that dysbindin may have a role in the regulation of depolarization-evoked DA release in the PFC and in the development of behavioral sensitization induced by repeated METH treatment.

© 2010 Elsevier Ireland Ltd. All rights reserved.

Schizophrenia is a devastating psychiatric disorder with a prevalence of 0.5–1.0%. Clinical symptoms are categorized into positive symptoms, negative symptoms, and cognitive dysfunction. Previous studies have suggested that dysfunction of dopaminergic (DAergic), glutamatergic, or GABAergic neurotransmission underlies the pathophysiology of schizophrenia [17]. Especially, hypofunction of the mesocortical DAergic system may be related to negative symptoms and cognitive dysfunction whereas hyperfunction of the mesolimbic DAergic system causes positive symptoms [5]. Serotonergic system is also implicated in features of schizophrenia since serotonin (5-HT)–dopamine (DA) antagonism by atypical antipsychotics can improve some positive and negative symptoms [25].

Dystrobrevin binding protein-1 gene (*DTNBP1*), which encodes dysbindin protein, has been identified as a schizophrenic associated gene through linkage and association analysis [28]. Postmortem brain studies have demonstrated that expression of dysbindin protein and mRNA are reduced in the PFC and hippocampus of schizophrenia [32,33]. Moreover, it has been demonstrated that a risk haplotype of *DTNBP1* in schizophrenia is associated with negative symptoms in schizophrenia [7].

Many studies have indicated that dysbindin contributes to the regulation of exocytosis and/or formation of synaptic vesicles. Dysbindin concentrates in the fraction containing enriched synaptic vesicle membrane [31]. Hikita et al. [11] demonstrated that dysbindin partially colocalizes with synaptophysin in primary cultured hippocampal neuron. Knockdown of dysbindin has affected the extracellular glutamate or DA levels in PC12 cells [16,22]. In addition to these *in vitro* studies, sandy (sdy) mouse has been available to study the physiologic function of dysbindin. Sdy mice arose from spontaneous mutation in a DBA/2J stock and carry a *Dtnbp1* allele encoding a protein with an in-frame 22-residue deletion [18]. Behavioral analysis revealed that sdy mice display impairments of cognitive function [1,30] and exhibit anxiety-related behavior

* Corresponding author at: Department of Neuropsychopharmacology and Hospital Pharmacy, Nagoya University Graduate School of Medicine, 65 Tsuruma-cho, Showa-ku, Nagoya 466-8560, Japan. Tel.: +81 52 744 2674; fax: +81 52 744 2979.
E-mail address: kyamada@med.nagoya-u.ac.jp (K. Yamada).
[1] Contributed equally to the work.

0304-3940/$ – see front matter © 2010 Elsevier Ireland Ltd. All rights reserved.
doi:10.1016/j.neulet.2009.12.071

[10]. Sdy mice have lower tissue content of DA in the cortex and hippocampus [19]. However, it remains to be determined if the regulation of neurotransmitter release in the brains of sdy mice is altered. In the present study, to investigate the molecular function of dysbindin in synaptic neurotransmission, we measured extracellular DA and 5-HT levels in the PFC of sdy mouse before and after depolarization stimulus, using *in vivo* microdialysis. In addition, we analyzed methamphetamine (METH)-induced hyperlocomotion and behavioral sensitization in sdy mice.

Sdy mice were obtained from the Jackson Laboratory (Bar Harbor, Maine, USA). The animals were housed in plastic cages and kept in a regulated environment (23 ± 1 °C, 50 ± 5% humidity), with a 12/12 h light–dark cycle (lights on at 9:00 a.m.). Food (CE2; Clea Japan Inc., Tokyo, Japan) and tap water were available ad libitum. All animal care and use were in accordance with the National Institutes of Health Guide for the Care and Use of Laboratory Animals and were approved by the Institutional Animal Care and Use Committee of Nagoya University.

For *in vivo* microdialysis, 11–18-week-old homozygous sdy mice ($n = 7$) and wild-type DBA/2J mice ($n = 6$) were anesthetized with sodium pentobarbital (50 mg/kg, i.p.) and a guide cannula (AG-4, Eicom Corp., Kyoto, Japan) was implanted in the PFC (+2.0 mm anteroposterior, −0.5 mm mediolateral from the bregma, −2.0 mm dorsoventral from the skull) according to the mouse brain atlas. On recovery from the surgery, a dialysis probe (A-I-4-01; membrane length 1 mm, Eicom Corp.) was inserted through the guide cannula, and perfused with artificial cerebrospinal fluid (aCSF, 147 mmol/l NaCl, 4 mmol/l KCl, and 2.3 mmol/l $CaCl_2$) at a flow rate of 1.0 μl/min. The outflow fractions were collected every 10 min. After the collection of baseline fractions, high potassium-containing aCSF (60 mM; isomolar replacement of NaCl with KCl) was perfused for 20 min through the dialysis probe. DA and 5-HT levels in the dialysates were analyzed using an HPLC system (HTEC-500, Eicom Corp.) equipped with an electrochemical detector [20]. The probe recoveries of DA and 5-HT were approximately 25%.

For measurement of locomotor activity, mice were placed individually in a transparent acrylic cage with a black frosting Plexiglas floor (25 cm × 25 cm × 20 cm), and locomotor activity was measured every 5 min for 60 min using digital counters with an infrared sensor (BrainScience Idea, Osaka, Japan). Wild-type and sdy mice were habituated to the test environment for 120 min before the measurement of locomotor activity. They were injected with saline or METH (0.5 or 1.0 mg/kg, s.c.), and the locomotor activity was measured for 60 min. For the behavioral sensitization, mice were injected with METH (1.0 mg/kg, s.c.) once a day for 5 days, and METH-induced locomotor activity was measured for 60 min.

All data were expressed as the mean ± S.E. Statistical significance was determined using a two-way analysis of variance (ANOVA) with or without repeated measures followed by the Bonferroni test when F ratios were significant ($p < 0.05$).

First of all, we studied the effect of depolarization stimulus on DA release in the PFC of sdy mice by *in vivo* microdialysis. As shown in Fig. 1, extracellular DA levels in the PFC of wild-type mice were increased by 60 mM KCl stimulation, and the KCl-evoked DA release was significantly diminished in sdy mice compared to wild-type mice [an ANOVA with repeated measures, genotype, $F_{(1,11)} = 8.130$, $p < 0.05$; time after the KCl treatment, $F_{(5,55)} = 37.810$, $p < 0.01$; genotype by time after the KCl treatment interaction, $F_{(5,55)} = 2.267$, $p > 0.05$]. Post hoc analysis revealed that depolarization-evoked DA release was markedly decreased in sdy mice compared with wild-type mice from 10 to 50 min after 60 mM KCl treatment ($p < 0.05$, Fig. 1). There was no difference in the basal levels of DA before the stimulation between the two groups (wild-type, 0.19 ± 0.04 pg/10 μl/10 min; sdy, 0.17 ± 0.02 pg/10 μl/10 min).

The mesocorticolimbic system is responsible for the locomotor-stimulating effects of METH. Therefore, we measured the

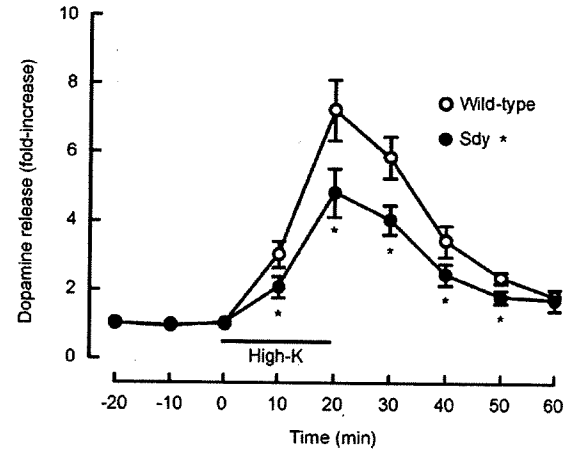

Fig. 1. Depolarization-evoked DA release in the PFC of sdy mice measured by *in vivo* microdialysis. A dialysis probe was inserted through the guide cannula, and perfused with an aCSF at a flow rate of 1.0 μl/min. Following the collection of three baseline fractions, high potassium-containing aCSF (60 mM KCl) was perfused for 20 min through the dialysis probe. Values represent the mean ± S.E. (wild-type, $n = 6$; sdy, $n = 7$). *$p < 0.05$ compared to the corresponding wild-type mice.

locomotor-stimulating effects of METH in sdy mice. Single METH (0.5 and 1.0 mg/kg s.c.) treatment induced hyperlocomotion in both wild-type and sdy mice [a two-way ANOVA, METH treatment, $F_{(2,42)} = 11.977$, $p < 0.01$, Fig. 2A]. There was no difference in the

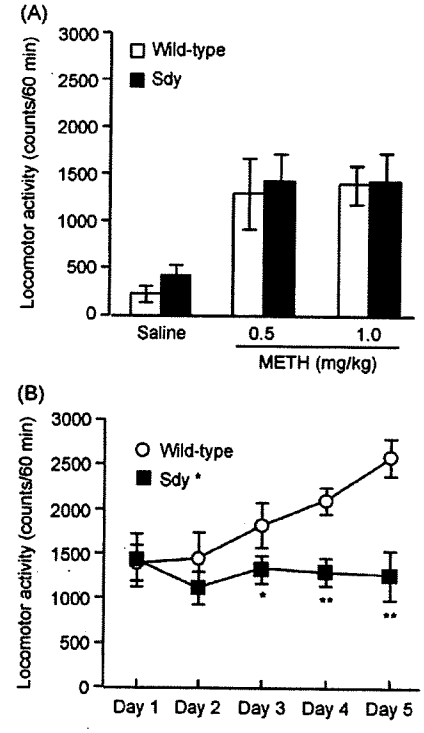

Fig. 2. METH-induced hyperlocomotion and behavioral sensitization in sdy mice. (A) Single METH-induced hyperlocomotion. Wild-type ($n = 7$ in each group) and sdy ($n = 9$ in each group) mice were habituated to the test environment for 120 min before the measurement of locomotor activity. Wild-type and sdy mice were injected with saline or methamphetamine (METH, 0.5 or 1.0 mg/kg, s.c.), and the locomotor activity was measured for 60 min. (B) Repeated METH-induced behavioral sensitization. Wild-type ($n = 7$) and sdy ($n = 9$) mice were habituated to the test environment for 120 min before the measurement of locomotor activity. Mice were injected with METH (1.0 mg/kg, s.c.) once a day for 5 days, and METH-induced locomotor activity was measured for 60 min. Values represent the mean ± S.E. *$p < 0.05$ and **$p < 0.01$ compared to the corresponding wild-type mice.

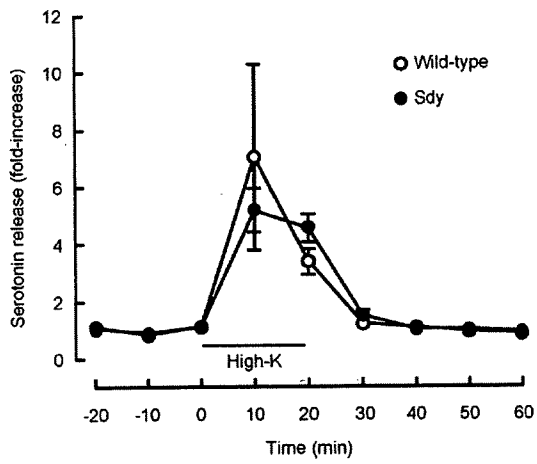

Fig. 3. Depolarization-evoked 5-HT release in the PFC of sdy mice measured by *in vivo* microdialysis. A dialysis probe was inserted through the guide cannula, and perfused with an aCSF at a flow rate of 1.0 μl/min. Following the collection of three baseline fractions, high potassium-containing aCSF (60 mM KCl) was perfused for 20 min through the dialysis probe. Values represent the mean ± S.E. (wild-type, $n = 6$; sdy, $n = 7$).

magnitude of METH-induced hyperlocomotion between wild-type and sdy mice at any doses examined [a two-way ANOVA, genotype, $F_{(1,42)} = 0.346$, $p > 0.05$; genotype by METH treatment interaction, $F_{(2,42)} = 0.046$, $p > 0.05$, Fig. 2A]. In wild-type mice, the locomotor-stimulating effect of METH was potentiated by repeated METH treatment (1.0 mg/kg/day, s.c.) for 5 days [an ANOVA with repeated measures: day after the METH treatment, $F_{(4,56)} = 4.346$, $p < 0.01$, Fig. 2B]. When the time course of METH-induced locomotor sensitization in sdy mice was compared with that in wild-type mice, the sensitization was found to be significantly decreased in sdy mice [an ANOVA with repeated measures: genotype, $F_{(1,14)} = 5.984$, $p < 0.05$; genotype by day after the METH treatment interaction, $F_{(4,56)} = 4.540$, $p < 0.01$, Fig. 2B].

We also investigated the role of dysbindin on the KCl-evoked 5-HT release in the PFC of mice (Fig. 3). Extracellular 5-HT levels in the PFC of wild-type mice were increased by 60 mM KCl stimulation. The KCl-evoked 5-HT release did not differ between wild-type and sdy mice [an ANOVA with repeated measures, genotype, $F_{(1,11)} = 0.010$, $p > 0.05$; time after the KCl treatment, $F_{(5,55)} = 11.921$, $p < 0.01$; genotype by time after the KCl treatment interaction, $F_{(5,55)} = 0.620$, $p > 0.05$]. Although the basal extracellular 5-HT levels were decreased in the PFC of sdy mice, there was no significant difference between the two groups (wild-type, 0.33 ± 0.11 pg/10 μl/10 min; sdy, 0.12 ± 0.01 pg/10 μl/10 min).

Single nucleotide polymorphisms in *DTNBP1* are associated with a reduced cognitive ability [2,3], lower scores on verbal, performance and fullscale IQ tests [34], and deficits in several tasks of attentional response control and/or working memory in schizophrenia [6]. It has been reported that DA content significantly decreased in the cortex, hippocampus and hypothalamus of sdy mice while its metabolite homovanillic acid does not differ between wild-type and sdy mice [19]. Furthermore, sdy mice have been shown to have larger vesicle size, slower quantal release and fewer release events in single cells of the adrenal gland and the hippocampus [4]. Taken together with our findings that the KCl-induced DA release was significantly decreased in the PFC of sdy mice compared with wild-type mice, it is plausible that dysbindin may have a role in the regulation of activity-dependent DA release in the PFC. Dysbindin also plays a role in DA receptor trafficking as shown by increased surface expression of D2 receptors in rat cortical neurons and human neuroblastoma cells following dysbindin siRNA treatment [12]. Presynaptic DA D2 receptors act as autoreceptors, which allow an inhibitory feedback mechanism by altering DA synthesis, release, and reuptake in response to increased synaptic DA. Accordingly, it is possible that decreased levels of extracellular DA in sdy mice may be due to the facilitation of negative feedback through DA D2 receptors in the presynaptic terminals.

Regarding the basal level of extracellular DA, there was no difference between two genotypes in our hands. However, it should be note that no-net flux method is preferred to determine a precise basal level of extracellular DA [23]. Therefore, further study may be required to clarify the role of dysbindin in basal DA release *in vivo*.

The DAergic neuronal activity in the mesolimbic system may be differently affected from that in the mesocortical DAergic system in schizophrenia. Accordingly, we are going to compare the changes in KCl-evoked DA release between the PFC and nucleus accumbens of sdy mice in future.

METH is substrate for DA transporter and competitively inhibits DA uptake and releases DA through reverse transport [27]. METH-induced elevation in extracellular DA leads to hyperlocomotion [27]. The DA efflux through DA transporter requires an increase in Ca^{2+}, and METH increase Ca^{2+} via release of Ca^{2+} from intracellular stores in a manner that is independent of changes in membrane depolarization [9]. Since there was no difference in single METH-induced hyperlocomotion between wild-type and sdy mice, it is unlikely that dysbindin plays a role in METH-induced DA release and hyperlocomotion.

In the present study, we found that repeated METH-induced behavioral sensitization, an animal model of METH psychosis, was significantly attenuated in sdy mice. Repeated treatment with amphetamine produces a persistent increase in the length of dendrites and the number of branched spines on medium spiny neurons [26]. An increase in mRNA levels of the synaptic proteins such as synaptotagmin IV and 25 kDa-synaptic-associated protein has been reported in the cortex, nucleus accumbens, striatum and hippocampus of rats after the repeated treatment with METH [14]. Interestingly, it has been demonstrated that dysbindin gene is associated with METH psychosis [15]. Thus, dysbindin may play a role in repeated METH-induced synaptic changes and DA release, which may underlie the sensitization of the locomotor-stimulating effect of the psychostimulant. Since activity-dependent synaptic plasticity and remodeling of the DAergic system play a crucial role in the development of repeated psychostimulant-induced behavioral sensitization [21], a role of dysbindin in such events should be elucidated in further research.

In contrast to DA release, KCl-induced 5-HT in the PFC of sdy mice did not differ from the release in wild-type mice, although a small reduction of basal extracellular 5-HT levels was observed. Accordingly, it is unlikely that dysbindin regulates the release of all neurotransmitters in the brain. It has been shown that knockdown of dysbindin results in a reduction of stimulus-induced glutamate release in primary cultured cortical neurons, suggesting that dysbindin may regulate release of glutamate [22]. Although it is unclear as to whether the specificity lies with DA and glutamate, it may be determined by the expression levels of as well as target proteins of dysbindin in the brain. A previous study demonstrated high levels of dysbindin mRNA in the substantia nigra and hippocampus in which DAergic and glutamatergic neurons, respectively, exist abundantly [33]. Furthermore, dysbindin is located on the synaptic vesicles, postsynaptic densities, and microtubules of apparent glutamatergic neurons in the hippocampus [32]. To our knowledge, there are no reports indicating the expression of dysbindin mRNA or protein in serotonergic neurons. This possibility should be the subject of further research.

Although the molecular mechanism by which dysbindin regulates depolarization-evoked DA release remains to be determined,

there are several possible explanations. It has been demonstrated that dysbindin binds to snapin [31], SNARE-associated protein implicated in neurotransmission [13]. Recent proteomic analysis has demonstrated that dysbindin directly interacts with Munc18-1 and AP3 complex [11]. Munc18-1 is a neuron specific protein that is essential for the exocytosis of synaptic vesicles [29]. In primary cultured hippocampal neurons, the disbindin-Munc18-1 protein complex is colocalized with synaptophysin [11]. Further studies including electophysiological analysis should be performed to verify the hypothesis that dysbindin may modulate depolarization-evoked DA release through the processes of exocytosis of synaptic vesicles.

Interestingly, disbindin has also been identified as a stable component of biogenesis of lysosome-related organelles complex 1 (BLOC-1) in the brain. The protein level of dysbindin is developmentally regulated, and the dysbindin-containing complex, BLOC-1, plays an important role in the neurite outgrowth [8]. Accordingly, it is possible that the developmental abnormality of DAergic neurons may lead to impaired depolarization-evoked DA release as within the developmental hypothesis of schizophrenia pathogenesis [24].

In conclusion, we demonstrated that depolarization-evoked DA release was diminished in the PFC of sdy mice, whereas KCl-evoked 5-HT release was unaffected. Repeated METH treatment led to the development of behavioral sensitization in wild-type mice, but not in sdy mice. Our findings suggest that dysbindin may have a role in the regulation of depolarization-evoked DA release in the PFC and in the development of behavioral sensitization induced by repeated METH treatment.

Conflict of interest

The authors declare that there are no conflicts of interest in the publication of the present work.

Acknowledgements

We thank Drs. N. Ogiso, Y. Ohya and K. Yano, Division for Research of Laboratory Animals, Nagoya University for their technical assistance. This study was supported in part by a Grant-in-Aid for Scientific Research (No. 19390062, 21790067) from the JSPS, Research on Risk of Chemical Substances, Health and Labor Science Grants supported by Ministry of Health, Labour and Welfare, the CREST from JST, the MEXT Global-COE Program, Academic Frontier Project for Private Universities; matching fund subsidy from MEXT, 2007–2011, Regional Joint Research Program supported by grants to Private Universities to Cover Current Expenses from MEXT, and grants from the Smoking Research Foundation.

References

[1] S.K. Bhardwaj, M. Baharnoori, B. Sharif-Askari, A. Kamath, S. Williams, L.K. Srivastava, Behavioral characterization of dysbindin-1 deficient sandy mice, Behav. Brain Res. 197 (2009) 435–441.
[2] K.E. Burdick, T.E. Goldberg, B. Funke, J.A. Bates, T. Lencz, R. Kucherlapati, A.K. Malhotra, DTNBP1 genotype influences cognitive decline in schizophrenia, Schizophr. Res. 89 (2007) 169–172.
[3] K.E. Burdick, T. Lencz, B. Funke, C.T. Finn, P.R. Szeszko, J.M. Kane, R. Kucherlapati, A.K. Malhotra, Genetic variation in DTNBP1 influences general cognitive ability, Hum. Mol. Genet. 15 (2006) 1563–1568.
[4] X.W. Chen, Y.Q. Feng, C.J. Hao, X.L. Guo, X. He, Z.Y. Zhou, N. Guo, H.P. Huang, W. Xiong, H. Zheng, P.L. Zuo, C.X. Zhang, W. Li, Z. Zhou, DTNBP1, a schizophrenia susceptibility gene, affects kinetics of transmitter release, J. Cell Biol. 181 (2008) 791–801.
[5] K.L. Davis, R.S. Kahn, G. Ko, M. Davidson, Dopamine in schizophrenia: a review and reconceptualization, Am. J. Psychiatry 148 (1991) 1474–1486.
[6] G. Donohoe, D.W. Morris, S. Clarke, K.A. McGhee, S. Schwaiger, J.M. Nangle, H. Garavan, I.H. Robertson, M. Gill, A. Corvin, Variance in neurocognitive performance is associated with dysbindin-1 in schizophrenia: a preliminary study, Neuropsychologia 45 (2007) 454–458.
[7] A.H. Fanous, E.J. van den Oord, B.P. Riley, S.H. Aggen, M.C. Neale, F.A. O'Neill, D. Walsh, K.S. Kendler, Relationship between a high-risk haplotype in the DTNBP1 (dysbindin) gene and clinical features of schizophrenia, Am. J. Psychiatry 162 (2005) 1824–1832.
[8] C.A. Ghiani, M. Starcevic, I.A. Rodriguez-Fernandez, R. Nazarian, V.T. Cheli, L.N. Chan, J.S. Malvar, J. de Vellis, C. Sabatti, E.C. Dell'angelica, The dysbindin-containing complex (BLOC-1) in brain: developmental regulation, interaction with SNARE proteins and role in neurite outgrowth, Mol. Psychiatry, in press.
[9] J.S. Goodwin, G.A. Larson, J. Swant, N. Sen, J.A. Javitch, N.R. Zahniser, L.J. De Felice, H. Khoshbouei, Amphetamine and methamphetamine differentially affect dopamine transporters in vitro and in vivo, J. Biol. Chem. 284 (2009) 2978–3289.
[10] S. Hattori, T. Murotani, S. Matsuzaki, T. Ishizuka, N. Kumamoto, M. Takeda, M. Tohyama, A. Yamatodani, H. Kunugi, R. Hashimoto, Behavioral abnormalities and dopamine reductions in sdy mutant mice with a deletion in Dtnbp1, a susceptibility gene for schizophrenia, Biochem. Biophys. Res. Commun. 373 (2008) 298–302.
[11] T. Hikita, S. Taya, Y. Fujino, S. Taneichi-Kuroda, K. Ohta, D. Tsuboi, T. Shinoda, K. Kuroda, Y. Funahashi, J. Uraguchi-Asaki, R. Hashimoto, K. Kaibuchi, Proteomic analysis reveals novel binding partners of dysbindin, a schizophrenia-related protein, J. Neurochem. 110 (2009) 1567–1574.
[12] Y. Iizuka, Y. Sei, D.R. Weinberger, R.E. Straub, Evidence that the BLOC-1 protein dysbindin modulates dopamine D2 receptor internalization and signaling but not D1 internalization, J. Neurosci. 27 (2007) 12390–12395.
[13] J.M. Ilardi, S. Mochida, Z.H. Sheng, Snapin: a SNARE-associated protein implicated in synaptic transmission, Nat. Neurosci. 2 (1999) 119–124.
[14] T. Isao, K. Akiyama, Effect of acute and chronic treatment with methamphetamine on mRNA expression of synaptotagmin IV and 25 kDa-synaptic-associated protein in the rat brain, Psychiatry Clin. Neurosci. 58 (2004) 410–419.
[15] M. Kishimoto, H. Ujike, Y. Motohashi, Y. Tanaka, Y. Okahisa, T. Kotaka, M. Harano, T. Inada, M. Yamada, T. Komiyama, T. Hori, Y. Sekine, N. Iwata, I. Sora, M. Iyo, N. Ozaki, S. Kuroda, The dysbindin gene (DTNBP1) is associated with methamphetamine psychosis, Biol. Psychiatry 63 (2008) 191–196.
[16] N. Kumamoto, S. Matsuzaki, K. Inoue, T. Hattori, S. Shimizu, R. Hashimoto, A. Yamatodani, T. Katayama, M. Tohyama, Hyperactivation of midbrain dopaminergic system in schizophrenia could be attributed to the down-regulation of dysbindin, Biochem. Biophys. Res. Commun. 345 (2006) 904–909.
[17] U.E. Lang, I. Puls, D.J. Muller, N. Strutz-Seebohm, J. Gallinat, Molecular mechanisms of schizophrenia, Cell Physiol. Biochem. 20 (2007) 687–702.
[18] W. Li, Q. Zhang, N. Oiso, E.K. Novak, R. Gautam, E.P. O'Brien, C.L. Tinsley, D.J. Blake, R.A. Spritz, N.G. Copeland, N.A. Jenkins, D. Amato, B.A. Roe, M. Starcevic, E.C. Dell'Angelica, R.W. Elliott, V. Mishra, S.F. Kingsmore, R.E. Paylor, R.T. Swank, Hermansky-Pudlak syndrome type 7 (HPS-7) results from mutant dysbindin, a member of the biogenesis of lysosome-related organelles complex 1 (BLOC-1), Nat. Genet. 35 (2003) 84–89.
[19] T. Murotani, T. Ishizuka, S. Hattori, R. Hashimoto, S. Matsuzaki, A. Yamatodani, High dopamine turnover in the brains of Sandy mice, Neurosci. Lett. 421 (2007) 47–51.
[20] T. Nagai, K. Yamada, M. Yoshimura, K. Ishikawa, Y. Miyamoto, K. Hashimoto, Y. Noda, A. Nitta, T. Nabeshima, The tissue plasminogen activator-plasmin system participates in the rewarding effect of morphine by regulating dopamine release, Proc. Natl. Acad. Sci. U.S.A. 101 (2004) 3650–3655.
[21] E.J. Nestler, Molecular basis of long-term plasticity underlying addiction, Nat. Rev. Neurosci. 2 (2001) 119–128.
[22] T. Numakawa, Y. Yagasaki, T. Ishimoto, T. Okada, T. Suzuki, N. Iwata, N. Ozaki, T. Taguchi, M. Tatsumi, K. Kamijima, R.E. Straub, D.R. Weinberger, H. Kunugi, R. Hashimoto, Evidence of novel neuronal functions of dysbindin, a susceptibility gene for schizophrenia, Hum. Mol. Genet. 13 (2004) 2699–2708.
[23] L.H. Parsons, A.D. Smith, J.B. Justice Jr., The in vivo microdialysis recovery of dopamine is altered independently of basal level by 6-hydroxydopamine lesions to the nucleus accumbens, J. Neurosci. Methods 40 (1991) 139–147.
[24] J.L. Rapoport, A.M. Addington, S. Frangou, M.R. Psych, The neurodevelopmental model of schizophrenia: update 2005, Mol. Psychiatry 10 (2005) 434–449.
[25] G. Remington, Alterations of dopamine and serotonin transmission in schizophrenia, Prog. Brain Res. 172 (2008) 117–140.
[26] T.E. Robinson, B. Kolb, Persistent structural modifications in nucleus accumbens and prefrontal cortex neurons produced by previous experience with amphetamine, J. Neurosci. 17 (1997) 8491–8497.
[27] R.B. Rothman, M.H. Baumann, Monoamine transporters and psychostimulant drugs, Eur. J. Pharmacol. 479 (2003) 23–40.
[28] R.E. Straub, Y. Jiang, C.J. MacLean, Y. Ma, B.T. Webb, M.V. Myakishev, C. Harris-Kerr, B. Wormley, H. Sadek, B. Kadambi, A.J. Cesare, A. Gibberman, X. Wang, F.A. O'Neill, D. Walsh, K.S. Kendler, Genetic variation in the 6p22.3 gene DTNBP1, the human ortholog of the mouse dysbindin gene, is associated with schizophrenia, Am. J. Hum. Genet. 71 (2002) 337–348.
[29] T.C. Südhof, The synaptic vesicle cycle, Annu. Rev. Neurosci 27 (2004) 509–547.
[30] K. Takao, K. Toyama, K. Nakanishi, S. Hattori, H. Takamura, M. Takeda, T. Miyakawa, R. Hashimoto, Impaired long-term memory retention and working memory in sdy mutant mice with a deletion in Dtnbp1, a susceptibility gene for schizophrenia, Mol. Brain 1 (2008) 11.